Master Thesis

Modeling of the euglycemic hyperinsulinemic clamp experiment using Bayesian inference

Written by *Fynn Frederic Wolf*

May 20, 2021

Supervised by
Kristian Moss Bendtsen and Ala Trusina

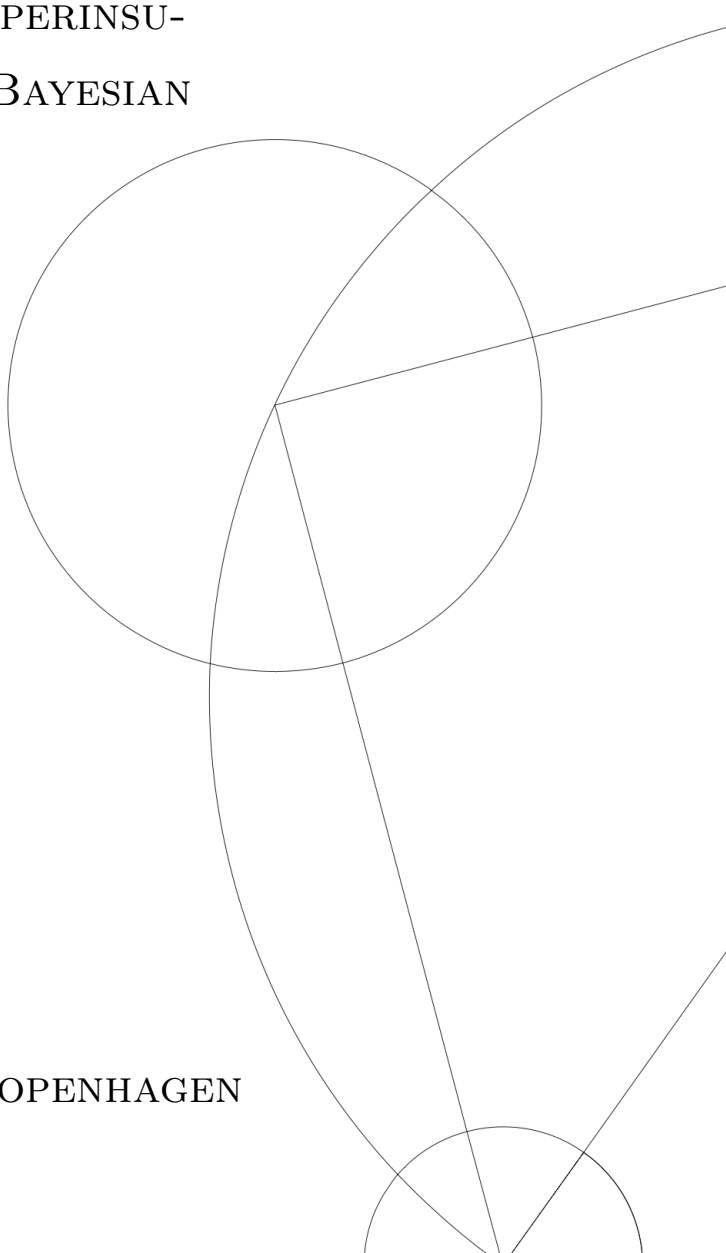

University of Copenhagen

UNIVERSITY OF COPENHAGEN

Faculty:	Faculty of Science
Institute:	Niels Bohr Institute
Author(s):	Fynn Frederic Wolf
Email:	mbc442@alumni.ku.dk
Title:	Master Thesis
Supervisor(s):	Kristian Moss Bendtsen and Ala Trusina
Handed in:	20.05.2021
Defended:	

Name _____

Signature _____

Date _____

Abstract

The glucose insulin system is well studied. Many mathematical models have been proposed and are capable of describing most of the workings of it. This thesis proposes a new model for the glucose insulin system and the euglycemic hyperinsulinemic clamp experiment using experimental data.

Experimental data from euglycemic hyperinsulinemic clamp experiments of rats for high and low insulin infusion rates suggest that the insulin removal rate follows a non linear dynamic. The model proposed in this thesis is based on this data. Motivated from the findings in the data new terms for the insulin and glucose removal have been derived. Initially a two-compartment model was used. To validate the model, it was attempted to fit it to the experimental data with a hierarchical model using Bayesian inference. Being unable to do so, the models complexity was reduced. With the reduced model it proved possible to model the insulin measurement of varying insulin infusion rates of the data and the tracer glucose of the euglycemic hyperinsulinemic clamp experiments and therefore capture the dynamics of the glucose removal. It was not possible to model the glucose observations of the experiment as a result of the model not being able to account properly for the endogenous glucose production. Analysis of the individual parameters however showed that the modeling of said observation was not due to the suggested model but due to the parameters adjusting to be able to describe the observations.

Acknowledgements

I would like to thank Kristian Moss Bendtsen, my supervisor from Novo Nordisk, who had the idea for this thesis and supported me throughout the thesis. Further I would like thank Novo Nordisk for letting me use their data for my thesis.
Also, I would like Ala Trusina, my supervisor from NBI, who always had calming words whenever I needed it. Further I would like to thank Ala Trusina's working group which always had good discussions a nice feeling in their meetings.
Furthermore, I would like to thank my friends and my family who supported at all times and never got sick of me and my complaints. Special thanks have to go to Katharina Hauer who was of great help to me during this periode.

Contents

1 Introduction

With the number diabetic people raising constantly, the importance of understanding the glucose insulin system increases. One of the most practiced experiments to investigate and quantify insulin resistance is the euglycemic hyperinsulinemic clamp experiment. The process of conducting the experiment is very a labour intensive one. The simple interpretation of the results, however, makes the effort worth [1]. For a better understanding of the insulin glucose system mathematical models are needed.
In this thesis, it is attempted to model the euglycemic hyperinsulinemic clamp experiment using Bayesian inference. A model of the insulin glucose system is proposed based on data of euglycemic hyperinsulinemic clamp experiment performed on rats. The data was provided by Novo Nordisk. The model tries to describe the insulin glucose system as good as possible with the provided data. Another model, a reduction of the first model, is proposed. The main purpose of this model is not to describe the insulin glucose system as good as possible but to have a more simple model that is able to describe the euglycemic hyperinsulinemic clamp experiment. The models are validated on data of experiments in a hierarchical structure using Bayesian inference. The goal was to find a probability distribution for each parameter.
In chapter 2, a biological background of the insulin glucose system is given. Chapter 3 introduces the methods used in this thesis. An overview over mathematical models, Bayesian inference, Markov Chain Monte Carlo and No-U-Turn Sample, and pharmacokinetics is given. Chapter 4 introduces the data, where first the experimental procedure of a euglycemic hyperinsulinemic clamp experiment and an IV experiment is given which is then followed by an overview of the data. Chapter 5 introduces the proposed models and discusses their validity by parameter estimation via Bayesian inference. Lastly in Chapter 6 a conclusion of the work in this thesis is given.

2 Biological Background

2.1 Insulin Glucose System

2.1.1 Insulin

Insulin is a peptide hormone that controls the blood glucose levels by its action on liver, kidney, adipose tissue and skeletal muscle. Its secretion from the β-cells of pancreatic islets of Langerhans is mainly dependent on the blood glucose levels even though other factors such as macronutrients, hormones, humoral factors and neural input can also stimulate insulin secretion. In addition to that a connection between insulin blood concentration and insulin secretion from the β-cells have been suggested. [3].
During the basal state insulin is continuously secreted at levels that allow for insulin-dependent cellular glucose uptake. Its secretion is stimulated by an increase of blood glucose. The secretion of insulin to stimuli happens biphasic. An initial rapid release of insulin, where already synthesized and stored insulin is released, is followed by a steadier

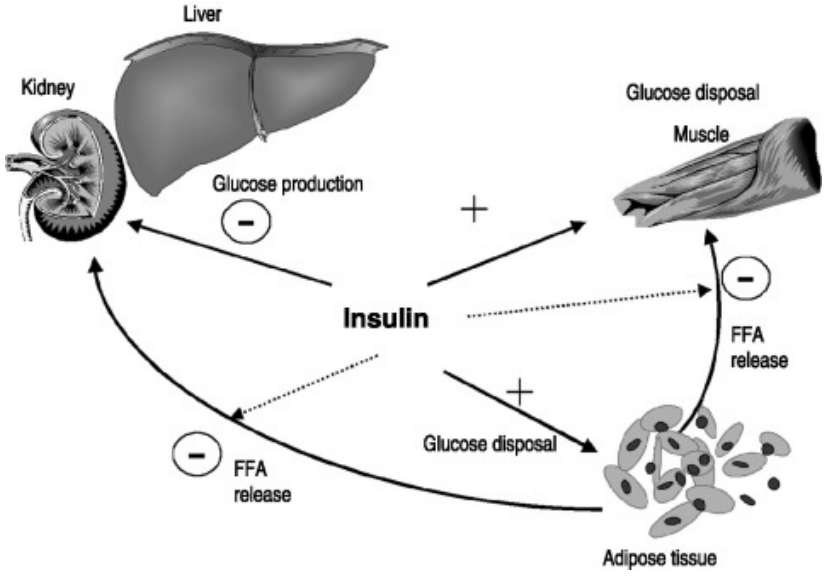

Figure 1: Effect of insulin on glucose production and disposal. The regulating effect of insulin towards glucose production and disposal is shown. Full arrows indicate a direct influence, dashed errors show an indirect influence. + and − denote the promoting and inhibiting effects of insulin on that system. Insulin directly inhibits the glucose production in kidney and liver. Further, insulin promotes the glucose disposal in muscle and in adipose tissue. Glucose disposal in adipose tissue decreases FFA levels which has inhibiting effect of glucose production in liver and kidney as well as an inhibiting effect of glucose disposal in muscle. Figure from from [2].

slower phase, where the secretion is a combination of both stored and newly synthesized insulin. The secreted insulin from the islet cells is released into the portal vein. From the portal vein insulin is carried to the liver where up to 80 % of it is cleared [4]. It follows that the insulin concentration in the peripheral circulation is therefore only a third of the insulin concentration of the portal vein. Besides hepatic insulin clearance there is also extrahepatic (peripheral) clearance of insulin by the kidney, muscle, and adipose tissue.[5] The effect of insulin itself on the secretion of insulin is variable. Depending on whether a body is insulin sensitive or not insulin can increase its own secretion or suppress it. [6]

Insulin main purpose lies in the regulation of the glucose homeostasis where it is the only hormone that lowers blood glucose. This is done through different mechanisms on liver, kidney, adipose tissue and skeletal muscle, see Fig.1. In liver and kidney the endogenous glucose production is suppressed by regulation of the rate-limiting key enzymes for gluconeogenesis (glucose-6-phosphatase and fructose-1,6-bisphosphatase) and glycogenolysis (glycogensynthase and phosphorylase). Simultaneously it increases the transcription of glucokinase which turns glucose into glucose-6-phosphate which promotes glycogenesis which is the basis for glycolysis and glycogen synthesis [7]. In muscles, adipose tissue and other insulin-sensitive tissues insulin binds to specific insulin receptors which trigger a signaling cascade. Upon that the glucose transporter protein GLUT4 migrates from the intracellular pool to the membrane where it increases the glucose uptake of insulin-stimulated cells several fold. In adipose tissue the increase in glucose transport leads over several steps to a decrease in free fatty acid (FFA) levels in the circulation which in turn further decreases the glucose production in liver and kidney as well as promotes uptake of glucose into tissue.[7][2]

2.1.2 Glucose

Glucose is an aldohexose. It is the predominant source of energy for the body. Different tissues in the body utilize different amounts of glucose. In basal state the human brain takes $\sim 50\%$, the splanchnic bed $\sim 25\%$ and the insulin dependent muscle tissue $\sim 25\%$ of glucose [9]. In rodents the distribution of glucose utilization is different. The brain only makes up $< 10\%$ of the basal glucose turnover. Under euglycemic hyperinsulinemic clamp conditions the utilization changes again. In that case $70 - 80\%$ of the glucose will be used up by muscle mass.

The means of how the body derives glucose depends on the 'state' of the body. The two states are the fasting state and the fed state. Fig.2 shows the glucose homeostasis in these two case. During the fasting state blood glucose is derived from endogenous

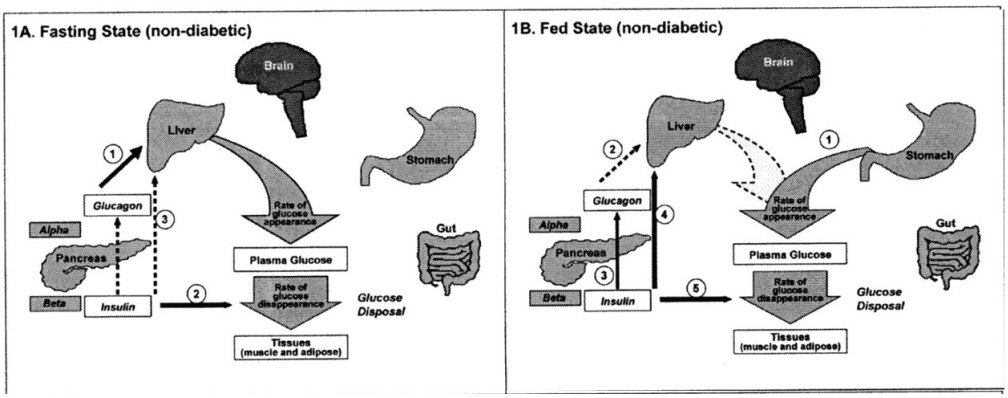

Figure 2: Glucose homeostasis. The role of insulin and gluacon are described for 1A fasting state and for 1B for the fed state in non-diabetic subjects. Full arrows indicate an active state while dashed arrows indicate an inactive state. 1A: In the fasting state no insulin is produced. Endogenous produced glucose is the only source for the plasma glucose. 1B: In the fed state insulin is produced in the β-cells of the pancreas. They suppress the endogenous glucose production. Glucose is taken up over the stomach. Figure from [8].

glucose sources. Approximately 50% of the glucose released into the circulation is produced by hepatic glycogenolysis. The remaining 50% is produced by glycogenolysis in the liver (30%) and the kidney (20%). Over a longer fasting period the fraction of glucose production shifts towards gluconeogenesis because glycogen stores in the liver are depleted rapidly. Insulin is able to suppress the glucose release from both processes. In the fed state blood glucose comes from the ingestion of nutrients in the stomach. During that time period endogenous glucose production is suppressed.[2]

Regulation of blood glucose levels is critical for the body. Both hypoglycemia (low blood glucose levels) and hyperglycemia (high blood glucose levels) are harmful for the body. Hyperglycemia can lead to life-threatening complications such as damage to the eye, kidney, nerves, heart and the peripheral vascular system [10]. On the other hand long term hypoglycemia can lead to loss of consciousness, disorientation, seizures and more [11]. A tight regulation of the blood glucose is therefore necessary.

Regulation of the blood glucose level is achieved by a combination of different mechanisms of which most involve the action of specific hormones by directing the glucose flux to and from glycogen store, balancing glycolysis and endogenous glucose production against each other as well as promoting protein catabolism. The two hormones that stand out because of their dominant and overriding actions in the regulatory system of glucose are insulin and glucagon [7]. Insulin production gets activated in response to

high blood glucose levels. Once released insulin binds to specific insulin receptors in muscles and other insulin sensitive tissues and triggers a signaling pathway. In response to that the glucose transporter protein GLUT4 is moved to the plasma membrane where it increases the glucose uptake into insulin-stimulated cells several fold. Other glucose transporter proteins such as GLUT1 work independent of the blood insulin concentration. GLUT1 is used by most brain cells to ensure that enough energy is provided even during fasting states where blood glucose and therefore also blood insulin levels are low [5]. Furthermore insulin promotes glycolysis and glycogenesis by increasing the amount of glucose 6-phosphate available. At the same time it inhibits the endogenous glucose production of the liver and the kidney. Glucagon on the other hand is produced in response to low blood glucose levels. It then promotes the release of glucose from glycogen. [7]

3 Methods

3.1 Models

Models are used to mathematically describe observed phenomena. While it is not only the goal to capture the variability of the observations y it is also desirable to have an underlying structural model f that approximates the physical phenomenon. Therefore it is most common to use nonlinear mixed effects models. With the addition of effects for the population and for individuals it is possible to use mixed effect models to describe a population.

3.1.1 Nonlinear Mixed Effect Models

The first part of nonlinear mixed effects models is the non linear part. This means the function f is free to choose whereas in a linear model f would need to be a linear function. The non linearity in our model allows for more physical relevant functions than linear functions would.
Our model is then defined as

$$y_j = f(t_j; \boldsymbol{\theta}) + e_j, \tag{3.1}$$

where y_j are our jth observation at time t_j, θ is vector of specific parameters for our model f and e_j is a vector of residual errors.
In many cases the function f is not defined directly but it is given as the solution of a system of ordinary differential equations (ODEs). For a lot of these systems there is no analytical solution and the function f can never be given. In these cases numerical solutions are used to solve the system of ODEs and the dependence of θ for f is only given in its ODE form.
Eq.3.1 only considers one individual. In many cases however the observations do not come from one, non-changing source. Even if the same event is observed there are almost always differences in the observations between each other. Capturing these differences is of interest to get a better understanding of the observed process. This can be achieved by using mixed effect models.
To capture the differences it can be assumed that the specific parameters θ can vary. For N different individuals we can therefore expend on Eq.3.1 and get

$$y_{ij} = f(t_{ij}; \boldsymbol{\theta_i}) + e_{ij}, \tag{3.2}$$

where y_{ij} is the jth individual of the ith observation, t_{ij} and e_{ij} are the corresponding time and residual error vectors, respectively, and θ_i is a vector containing the specific parameters for individual i.
Since the model is supposed to describe the same process but for observations that differs for whatever reasons it can be said that each parameter θ_{ik} can be displayed as a nonlinear function of a fixed effect β_k, an individual/random effect η_{ik} and covariates c_i, yielding

$$\theta_{ik} = h(\beta_k, \eta_{ik}, c_i). \tag{3.3}$$

Another way of non linearity occurs if the residual error is allowed to change between individuals. The change may occur between subjects or even possibly over time and can be modeled as a function g. Fig.3 shows some data with two different values for g. The upper one shows $g = a = const.$ and is called a constant error model. The error is the same for all values. Contrary to that is the error model shown in lower part of Fig.3. It shows a proportional error with $g = bf$. The error in that case is dependent on the value of the function.
Implementing all of these features yields,

$$y_{ij} = f(t_{ij}; \beta_k, \eta_{ik}, c_i) + g(t_{ij}; \beta_k, \eta_{ik}, c_i)e_{ij}. \tag{3.4}$$

3.1.2 Hierarchical models

Many models include parameters that are related to each other. For example consider a model that uses the heights of humans as a parameter θ_j. It would be reasonable to assume that the heights are related to each other. The dependency of these parameters can be reflected by a joint probability model. This can be achieved in a simple and natural way if a prior distribution is used for the related parameters. In that case the related parameters can be seen as samples from a common population distribution.
From that it follows that a population can be described by the same parametric, structural model f with different individuals, specific parameter vectors θ_i. This gives it a hierarchical structure that is a direct extension of the individual approach. The observations y_{ij} are modeled by parameters θ_i which themselves follow a given probabilistic specification determined by further parameters, so called hyperparameters.

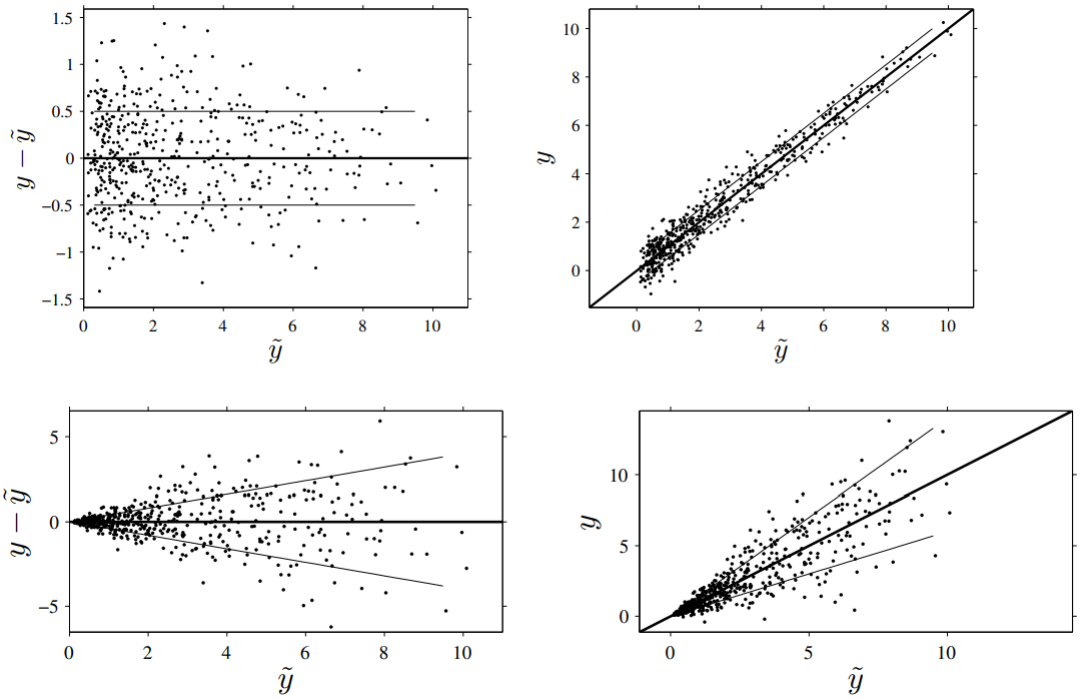

Figure 3: Constant and proportional error model. Upper figures show the a constant error model. The left figure shows the prediction error $y - \tilde{y}$ vs the prediction $\tilde{y}$. The left side shows the observations y_{ij} vs the predictions $\tilde{y}_{ij}$. The lines are $y = \tilde{y}$ and ± 1 standard deviation. Constant error models are used if the error is the for all measurements. Lower figure show the proportional error model. The figures follow the figures above. Proportional error models are used if the error in measurements increase with value. From [12].

The model can then be written as

$$y_{ij} = f(t_{ij}; \boldsymbol{\theta_i}) + e_{ij} \tag{3.5a}$$

$$\theta_i = h(\beta, \eta_i, c_i). \tag{3.5b}$$

where θ_i is the vector containing the specific parameters for observation i as a function of the hyperparameters β, η_i and c_i which are the fixed effects, the individual/random effects and the covariates, respectively.

A different way of describing Eq.3.5 is by using definitions. Using definitions is a more natural way of describing the distribution of the individual parameters. It is of more interest to describe the distribution of the individual parameters than it is of the distribution of random effects. Equations are not able to describe these distributions. They use 'artificial' random effects to mimic them. Additionally it is not possible to write all

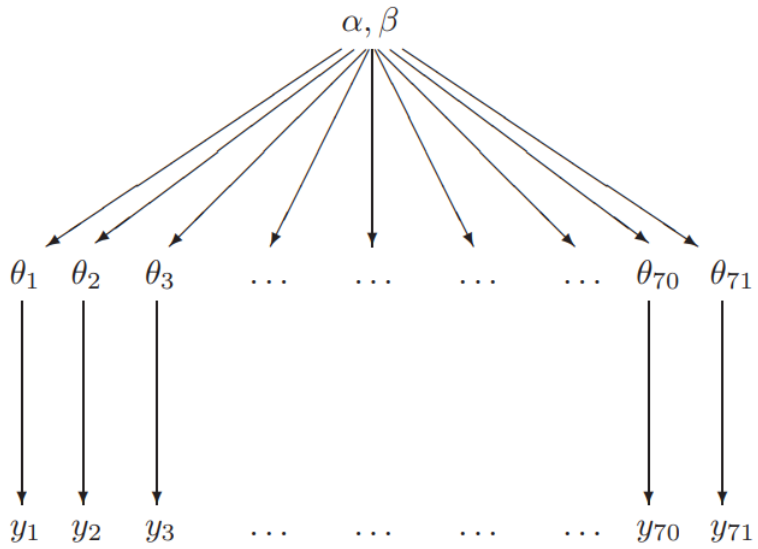

Figure 4: Visualization of the structure of a hierarchical model. Shared priors α and β allow for individual θ_i's that are used to describe individuals y_i's .From [13]

distributions as equations, e.g. categorical parameter, which limits their use further.
If the residual errors and random effects are mutually independent and normally distributed they can be written as follows,

$$e_{ij} \underset{\text{i.i.d.}}{\sim} \mathcal{N}\left(0, \sigma^2\right) \tag{3.6a}$$

$$\eta_{ik} \underset{\text{i.i.d.}}{\sim} \mathcal{N}\left(0, \omega_k^2\right). \tag{3.6b}$$

With these Eq.3.5 can be rewritten as

$$y_{ij} \sim \mathcal{N}\left(f(t_{ij}; \theta_i), \sigma^2\right) \tag{3.7a}$$

$$\theta_{ik} \underset{\text{i.i.d.}}{\sim} \mathcal{N}\left(h(\beta, c_i), \omega_k^2\right). \tag{3.7b}$$

The distributions are not limited to Gaussian distributions.

3.2 Bayesian Inference

The aim of Bayesian inference often is to find posterior predictive distribution of parameters $p(\theta|y)$ or unobserved data $p(\tilde{y}|y)$. The probability statements are given conditionally on the observed data y and implicitly conditionally on the known values of any covariates x.
To make this statement it is first necessary to have a model that provides a joint probability distribution for θ and y. That model is given by product of the prior distribution

$p(y|\theta)$ and the sampling/data distribution $p(y)$,

$$p(\theta, y) = p(\theta)p(y|\theta). \tag{3.8}$$

Using Bayes theorem, conditioning on the known values of the data y, yields the posterior density,

$$p(\theta|y) = \frac{p(\theta, y)}{p(y)} = \frac{p(\theta)p(y|\theta)}{p(y)}. \tag{3.9}$$

Since $p(y)$ does not depend on θ and can therefore be considered a constant. In that case it can be neglected, yielding the unnormalized posterior density,

$$p(\theta|y) \propto p(\theta)p(y|\theta). \tag{3.10}$$

Even though $p(y|\theta)$ is the conditional probability of y given θ it is in the circumstances taken as function of θ and not of y.
These equation are the technical core of Bayesian inference. Developing an appropriate model $p(\theta, y)$ and using computations, such as samplings, to find $p(\theta, y)$ is the goal of this method. Further information about the program used for Bayesian inference in this work can be found in Appendix C.

3.3 Pharmacokinetics

The goal of pharmacokinetics is the study of drug absorption, distribution and elimination inside a body. While there is also an experimental part of pharmacokinetics this chapter will only focus on the mathematical approach to it. It is of interest to try and describe these processes in a quantitative way using mathematical models. This section follows [14].

3.3.1 One-Compartment Model

The easiest way of doing so is by using a one-compartment open model with an intravenous injection (IV bolus). One-compartment means that the whole body is considered as one compartment. Everything that happens in the model happens in that one compartment. The open refers to the possibility of drugs to enter and the leave said compartment. The IV bolus means that the drug is immediately in the blood stream and eliminates the absorption part. Only distribution and elimination are left. Upon injection the drug is considered to be distributed homogeneously throughout the

compartment instantaneously. The elimination of the drug starts immediately after injection. While this model is very simplistic in its nature it can still be useful in the description and prediction of drug disposition.
In reality when a drug is injected intravenously the drug enters the blood stream and distributes through the blood circulation throughout the body. This is a rapid process and can be assumed as instantaneous in most cases. The distribution from the blood circulation to other tissues is in most cases a slower process. The rate the drug is distributed at through a specific tissue depends on several processes and properties, for example the blood flow in that tissue, the ability to enter the tissue from the blood stream and the affinity of the tissue for the drug.
If the uptake processes are fast enough that complex system can be reduced to a one compartment system. The volume of that system is called apparent volume of distribution V_D. It has no physiological meaning since no such compartment exists but it is assumed that the injected drug will distribute homogeneously in that volume. It is a theoretical volume, similar to the theoretical compartment, that gives the proportion between the amount of the drug in the body D_B and the concentration of the drug in the blood plasma C_p,

$$D_B = V_D C_P. \tag{3.11}$$

Drug elimination happens most of the time in multiple places at the same time, for example by liver metabolism and renal excretion. Both of these processes can be described with as first-order elimination with constants k_m and k_e, meaning they depend on the amount of drug in the compartment linearly. These are the most common rates in pharmacokinetics. All first-order elimination rates in any compartment can be summarized into one first-order elimination rate k describing the elimination of the drug from that

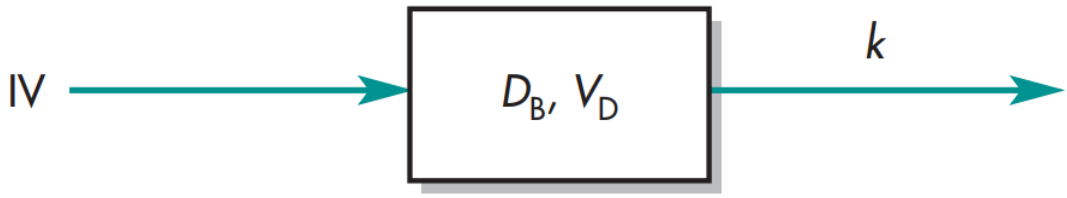

Figure 5: One-compartment model. Structure of a one-compartment model with an IV bolus injection and one removal. D_B is the amount of drug in the body, V_D is the apparent volume of distribution and k is the elimination rate constant. From [14]

compartment,

$$k = k_m + k_e. \tag{3.12}$$

That one-compartment model with two eliminations and one IV bolus at time $t = 0$ can then be written as

$$\frac{dD_B}{dt} = -kD_B. \tag{3.13}$$

The solution to this equation can be derived analytically. The slope is given by the first-order elimination rate k and the intercept with the y-axis is given by the initial amount of drug D_B^0 injected into the body.
Since measurements measure the blood plasma concentration of the drug C_D and not the amount of drug in the body D_B it is useful to have Eq.3.13 in concentrations. This can be achieved by substituting Eq.3.11 into Eq.3.13,

$$\frac{dC_P}{dt} = -kC_P. \tag{3.14}$$

Similar to above, Eq.3.14 can be solved analytically. The difference of the solution of Eq.3.13 would only be in a scaling factor. Since the distribution between plasma and tissue is assumed to be fast the concentration of the plasma is at any time proportional to the concentration of the tissue. It follows that any decline in plasma concentration is therefore proportional to the declines/removal in tissue. This allows the one-compartment model to be useful for predicting concentrations of the blood plasma even though it is only a very simple approximation.

3.3.2 Clearance

The measure of the drug elimination from the body without identifying the underlying mechanism or process is called clearance Cl. Clearance refers to the fraction of drug inside the body that is removed per unit time. It might also be considered as the volume of plasma fluid that is cleared of drug per unit time. Describing clearance in different ways grants different levels of insight and application in pharmacokinetics.
For first-order elimination processes clearance is a constant. Taking Eq.3.13 and substituting D_B on the left hand side with Eq.3.11 yields,

$$\frac{dD_B}{dt} = -kC_P V_D. \tag{3.15}$$

Dividing both sides by C_P gives the clearance Cl as volume of plasma fluid that is cleared of drug per unit time,

$$\frac{dD_B/dt}{C_P} = -kV_D = -Cl. \tag{3.16}$$

To get the fractional clearance of the drug one only needs to divide by the apparent volume of distribution V_D. Expressing the clearance Cl in terms of fractions over time has the benefit of independent on whether the measurements are in concentrations or amounts. For first-order processes this is directly incorporated in pharmacokinetics with the elimination rate constant k.

3.3.3 Non Linear Pharmacokinetics

In the previous chapters elimination of any drug was considered to be a linear first-order process. However, for some drugs higher dosages can cause deviations from the linear first-order elimination.

The processes of absorption, distribution and elimination can involve enzymes or carrier-mediated processes in a lot of cases. These processes can get saturated if the drug is provided in big enough quantities. Besides through saturation processes nonlinear be-

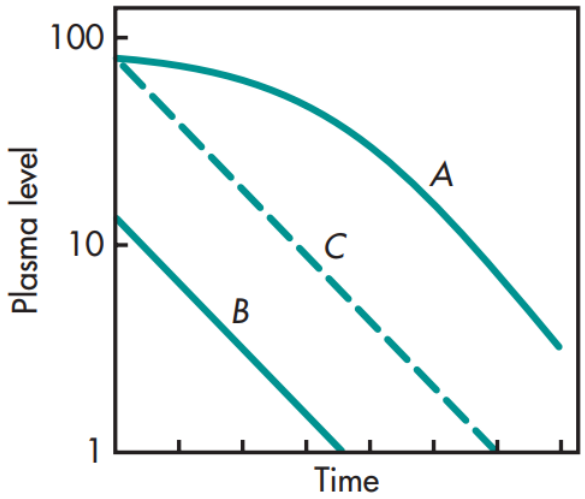

Figure 6: Non linear clearance of plasma levels. A and B show plasma level curves for a saturable elimination process. A presents a high dose, B presents a low dose. Curve A shows a non linear clearance for high values. The terminal slope of A and B are identical. Curve C shows a linear removal for a high bolus. Curves A and C highlight the difference between non linear clearance and linear clearance. From [14]

haviour can occur due to pathological alteration in some of these processes.
A drug that follows saturation kinetics has most of the time some tells. The drug does not follow first-order elimination processes, the half-life of the drug changes with changes in the dose, the saturation of capacity limited processes might be affected by other drugs that use the same enzyme or carrier-mediated system and the composition of the metabolites of a drug might be affected by a change in the dose. As a lot of these drugs only show these behaviours for large doses it can be difficult to make predictions based on small doses. Even though these saturation effects are present in some drugs it is not always necessary to model them if the drugs are only present at lower levels where they follow first-order elimination processes in approximation as can be seen in Fig.6.
Saturable elimination processes are described by Michaelis-Menten kinetics. The elimination rate is then given by

$$\text{Elimination Rate} = \frac{dC_P}{dt} = \frac{V_{max}C_P}{K_M + C_P}, \tag{3.17}$$

with V_{max} being the maximum elimination rate and K_M being the Michaelis-Menten constant. The Michaelis-Menten constant defines the concentration of C_P that is necessary for an increased removal. From Eq.3.17 it can also be seen that for $C_P = K_M$ the removal is at its half maximum. The values of these two parameters, V_{max} and K_M, depend on the drug as well as the enzymatic or carrier-mediated process.
Eq.3.17 describes the case if C_P covers a broad range. For the limits of C_P that expression can be simplified. For $C_P \ll K_M$ the elimination rate simplifies to,

$$\text{Elimination Rate} \approx \frac{V_{max}C_P}{K_M} = \hat{K}C_P, \tag{3.18}$$

a first order elimination process with the elimination rate $\hat{K} = V_{max}/K_M$ as mentioned above.
For $C_P \gg K_M$ Eq.3.17 gives,

$$\text{Elimination Rate} \approx \frac{V_{max}C_P}{C_P} = V_{max}, \tag{3.19}$$

a constant, saturated elimination which is why Michaelis-Menten kinetics were chosen.

3.3.4 Multi-Compartment Model

Multi-Compartment models are an extension to one-compartment models. As drug absorption, distribution and elimination inside a body are complex processes a one-compartment model is often not sufficient to describe these. Similar to the one-compartment

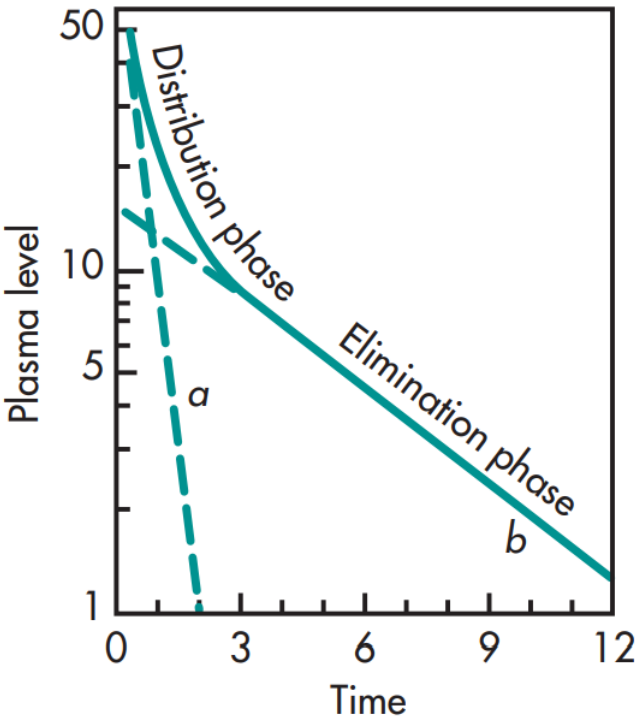

Figure 7: Biphasic removal. Plasma level curve of a two-compartment model showing a biphasic removal. Biphasic because the removal can be separated into two phases, a distribution phase and a elimination phase. Both follow a linear removal shown by a and b resulting in a non linear removal. From [14]

model it is assumed in the multi-compartment models that the drug concentration C_t is uniform and is distributed rapidly within any compartment. While in the one-compartment model everything inside the body is described by one compartment the multi-compartment model can make more separation between the different systems in our body. It is common to have a central compartment that describes the blood, extra-cellular fluid, and highly perfused organs/tissues such as heart, liver, and kidneys where the drug is distributed from to other peripheral compartments, i.e. a tissue compartment that represents the muscle mass and connective tissue. The drug concentration in the tissue compartments C_t is only theoretical since drug concentration in the body varies between different types of tissues and sometimes even within one type of tissue. However the drug concentration C_t may represent the average drug concentration over the different tissues. It follows that these concentrations can not be used to confirm or forecast actual tissue drug levels.

In many cases the curve after an IV bolus does not look like the mono-exponential

decay described in the one-compartment model but it declines in a biphasic fashion as demonstrated in Fig.7. A fast initial decline is followed by a more moderate one some time afterwards. The first decline phase is referred to as distribution phase. In that phase the drug is distributed from the central compartment, where the injection happened, to all the other compartments. The drug transfer between the compartments is taken as a first-order process. With time an equilibrium is formed between the fraction of drug in the tissue compartments and in the central compartment where the central compartment reflects proportional changes in all the other compartments. At that point the second, more moderate decline phase is active. It is called the elimination phase. In this phase the driving cause is the elimination of the drug from the body. Any elimination in the tissue compartments are reflected proportional in the central compartment. Because of that it appears as if the drug kinetics follow a one-compartment model.
Fig.8 shows possible two-compartment models. k_{12} and k_{21} are the rate parameters from the first-order process of the drug transfer between the compartments. The ratio k_{12}/k_{21} between them determines how the concentration in the equilibrium is distributed between the two compartments. k_{10} and k_{20} are elimination rates from the central and the peripheral compartment, respectively. As in one-compartment models they can also take a non linear form. As Fig.5 shows elimination of the drug can happen in either one or both of the compartments. If no further information about the drug is known then elimination from the central compartment is assumed as the major sites of drug elimination, such as kidney and liver, are located there.

The model in Fig.8A can be written as

$$\frac{dC_c}{dt} = -k_{12}C_c + k21C_p - k_{10}C_c \tag{3.20a}$$

$$\frac{dC_p}{dt} = k_{12}C_c - k_{21}C_p, \tag{3.20b}$$

with C_p and C_t being the drug concentration in the central and the peripheral compartment respectively, k_{12} and k_{21} being the first order transfer rates and k_10 being a first order elimination rate from the central compartment.
Following the one-compartment model each compartment of the multi-compartment model has its own volume of distribution. Following Eq.3.11 they are defined as

$$C_c = \frac{D_c}{V_c} \tag{3.21a}$$

$$C_p = \frac{D_p}{V_p}, \tag{3.21b}$$

with C_c, C_p being the concentrations, D_c and D_p being the amounts of drugs V_c and V_p being the volumes of distribution in the central and peripheral compartment, respec-

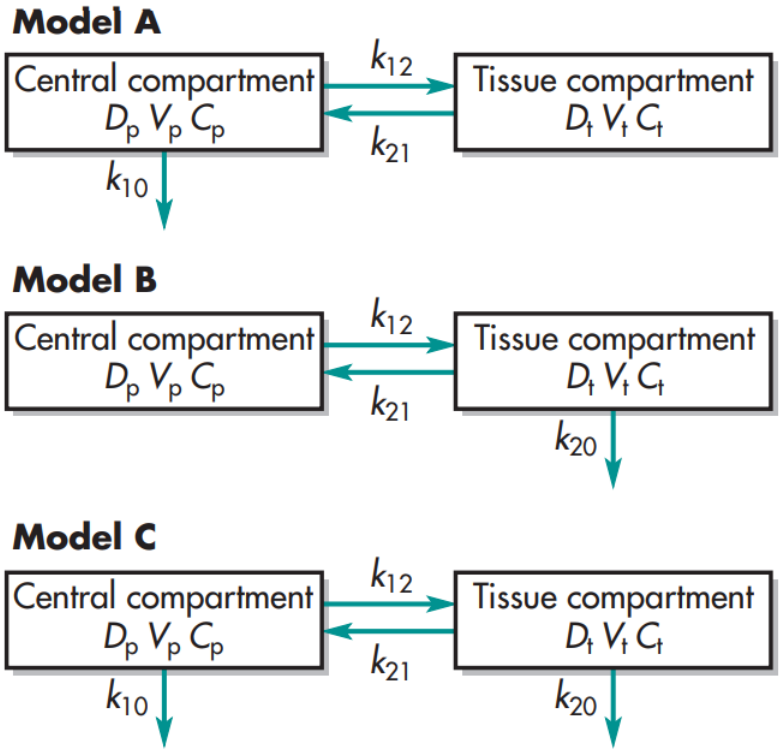

Figure 8: Two-compartment open models. Three ways a two-compartment model could be defined as. All three models contain a central and tissue compartment. D_i, V_i, and C_i are the amount of drug, the apparent volume of distribution and the drug concentration, respectively, for the central p and tissue t compartment. All three models have a linear transfer rates k_{12} and k_{21} between the compartments. Model A has elimination from the central compartment, Model B from the tissue compartment and Model C from both compartments. Elimination rates are given by k_{10} and k_{20} for the central and peripheral compartment, respectively. From [14]

tively.

In accordance to Eq.3.13 and Eq.3.14, Eqs.3.20 can be written in terms of drug amounts using Eqs.3.21 yielding,

$$\frac{dD_c}{dt} = -k_{12}D_c + \hat{k}_{21} - k_{10}D_c \tag{3.22a}$$

$$\frac{dD_p}{dt} = \hat{k}_{12}D_c - k_{21}D_p, \tag{3.22b}$$

with $\hat{k}_{21} = k_{21}V_c/V_p$ and $\hat{k}_{12} = k_{12}V_p/V_c$.

3.3.5 A priori Identifiability

A priori identifiability is to determine whether it is possible to estimate the parameters of a postulated model under perfect conditions of noise-free measurements and error-free model structure. Knowing that a model is *a priori* identifiable does not mean that the parameter estimation from real data is possible or that the model itself is correct.
Finding out if a linear or nonlinear model is identifiable is a difficult task. There exists no solution for the general case. Only a few specific linear and nonlinear models have been solved. Different methods such as transfer function, normal mode, exhaustive modelling, power series expansion and differential algebra are used to find out if a model is *a priori* identifiable or not.
Any model can be globally uniquely identifiable, locally nonuniquely identifiable or unidentifiable. In the first case all parameters are uniquely identifiable. This means that any parameter p_i of the model has only one solution. Locally nonuniquely identifiable means that all parameters p_i are identifiable, either uniquely or nonuniquely. A parameter is considered nonuniquely if it has more than one but a finite number of solutions. An unidentifiable model is considered if at least one parameter is unidentifiable. This means any parameter p_i has an infinite number of solutions.[15] [16]
A model where the *a priori* identifiability has been determined is the two compartment model with linear elimination. The three possible configurations of the model are displayed in Fig.8. Of these three models the rate constants of model A and B are uniquely identifiable whereas the for rate constants of model C are unidentifiable [17].

4 Data

As a base and a verification of the proposed models in this work, experimental data is used. The data is provided by Novo Nordisk. The data is based on rat studies performed by Novo Nordisk. Two types of studies were performed to create the four data sets provided, clamp studies and IV studies. The clamp studies can be further separated into normal clamp studies and clamp studies with the addition of tracer glucose. Similar, the IV studies can be divided into insulin IV studies and tracer glucose IV studies. The provided data is therefore given by four data sets with two for each study type. For each study type, tracer studies have been performed. As these are Each data sets contains a minimum of two studies, with each study containing multiple experiments.
In this chapter, first the experimental protocol of the clamp study and the IV study will be explained. Afterwards the data gathered during the experiments will be described and analysed.

4.1 Glucose Clamp and IV Studies

There are two main motivations behind doing euglycemic hyperinsulinemic clamp experiments. One motivation is that glucose clamp experiments are required in the regulatory guidelines for the development of new insulin analogs. Since Novo Nordisk is a company that produces insulin analogs and develops new ones these studies are very common. The first and largest data set stems from these kind of studies. As a support to these studies IV bolus experiments were conducted. These IV bolus experiments were used to test at what time scale the insulin analog is acting. The data from these experiments form one of the data sets. The second motivation for euglycemic hyperinsulinemic clamp experiments is to asses pharmacodynamic characteristics of insulin analogs. These studies are also present in the data set. They form the second euglycemic hyperinsulinemic clamp studies. The difference between these experiments and normal one is that in these tracer glucose is used. The addition of tracer glucose allows for a better tracking of glucose and therefore offers more information about the dynamics of the glucose inside the body. Similar as in the first glucose clamp study an IV bolus experiment was conducted for this study. In this case the bolus was done with tracer glucose to get more information about the dynamics of glucose inside the body. IV bolus experiments for insulin analogs are not necessary because the experiments were preformed with already known insulin.
Glucose clamp experiments are based on the concept that the blood glucose lowering effect of insulin is counteracted by a controllable infusion of glucose. The goal is to get

the plasma glucose level of the rat to a target value and hold it there in steady state. The experimental implementation follows these concepts pretty directly. The subject, here rats, is equipped with two IVs, one for glucose and one for insulin infusion. Through the insulin IV the rat is given a constant infusion of insulin for the whole duration of the experiment. In some cases a bolus is administered at the start of the experiment in addition to the normal infusion rate to get slow acting insulin analogs started. The glucose IV is then used to inject a glucose infusion. This glucose infusion rate (GIR) is controlled by the laboratory worker. The laboratory worker is free to change the infusion rate at will to get the plasma glucose levels near the target value. To make this possible the plasma glucose level of the subject is measured every ten minutes. To support the ability of the laboratory worker to get the glucose plasma levels close to the target value the movement of the subject is tracked. This is done by a string that

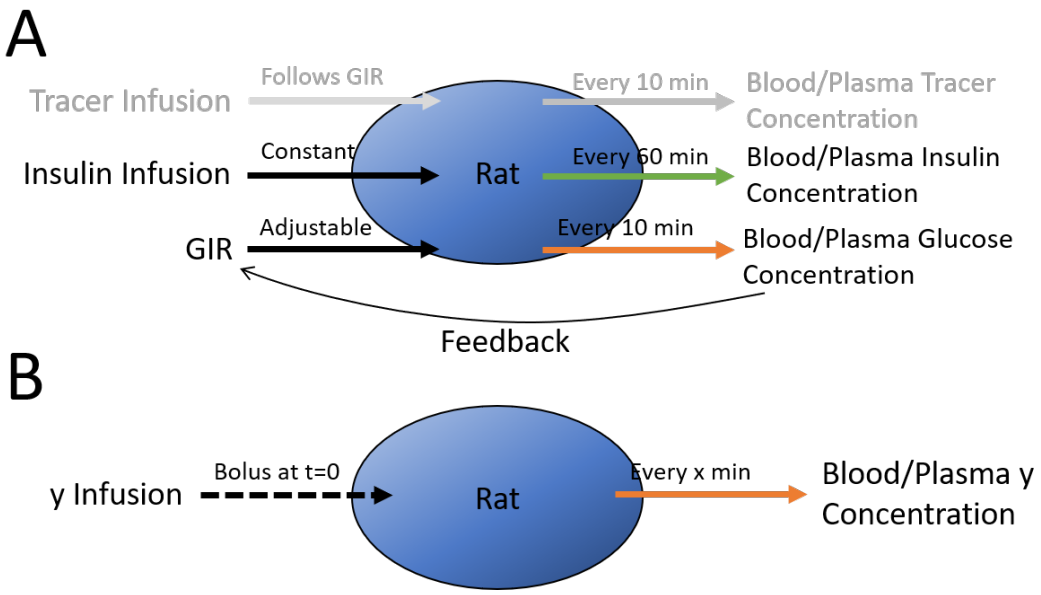

Figure 9: Illustration of clamp and IV experiment. Arrows on the left side indicate an input, arrows on the right side an output. A shows a clamp experiment. Over the whole experiment insulin and glucose are infused. Insulin has a constant infusion rate whereas the GIR is adjusted by the experimentalist. Every 10, 60 min the blood/plasma glucose, insulin concentration is measured. Glucose measurements are evaluated immediately and used as a feedback for the GIR. Additionally tracer glucose can be infused and measured. The tracer infusion rate follows the GIR. B shows an IV experiment. A bolus is injected a $t = 0$ and every xmin a the blood/plasma concentration is measured. Typically measurements are more frequent in the beginning and less frequent in the end.

is placed into the neck of the subject. Whenever the subject moves the string lengthen or shorten. This change in length is tracked, documented and given to the laboratory worker. The setup for the clamp experiments with tracer glucose is pretty much similar. There are still only two IV's. The tracer glucose will be given to rat over the same IV as the normal glucose. A small fraction of the glucose is equipped with tracers. The tracer glucose therefore always follows the GIR. 90min before the experiment starts a bolus of tracer glucose will be given to the subject.
The setup for the IV experiments is much simpler. The subject is given a bolus of insulin or tracer glucose via the appropriate IV and the plasma concentration of either is measured at certain times. There are some differences in the execution of the experiments between the two. Even between the different studies for the insulin IV there are differences. In some studies the subjects were anaesthetized while in most other studies they were not. Another factor that can differ between studies is if they measured the insulin levels in the blood or in the plasma. For the glucose measurements there are only two studies, both of them were conducted in the same way. On the contrary to the insulin measurements the movement was tracked for theses measurement.

4.2 Data Structure and Data Analysis

As all data sets are provided by Novo Nordisk and as they are used to provide different information for this work there are some general structures all of the data sets have in common as well as a few that distinguishes them. For the different experiments to be able to support each other it is necessary for them to be comparable. It follows therefore that the subjects of each experiment, the rats, and the methodology applied in the individual experiments should be as similar to each other as possible. As mentioned above, only two types of experiments have been performed, IV and clamp studies. Most noteworthy is, that all studies were performed on male Sprague Dawley rats.
Each experiment is labeled by an ID and a study. Every study has a unique identification and every experiment within a study has an ID that is unique for the study. ID's between studies can be identical. For each experiment the following information about the rat were given: strain, sex, fasted or fed, weight and anaesthetized or not. As mentioned before, the strain and sex of the rat was identical in all cases. The other data varies between experiments. In addition to the data concerning the subject every data set gives notice of whether the blood or the plasma concentrations were measured. For simplicity reasons they will be referred to as blood concentrations throughout this work. For data sets containing insulin measurements the batch number of the used insulin is provided. The batch number contains information about the type of insulin and in which batch it

was synthesized. What further data is provided depends on the data sets.
Besides these information each experiment contained the data of the measurements. In the following sections this data will be described and further analysed.

4.2.1 IV Data

Each measurement in each experiment is given by a time series, a concentration series and the bolus amount. The insulin IV studies have measurements for both glucose and insulin while the glucose tracer IV measurements only contains measurements of the glucose tracer concentration. Only the insulin measurements are of interest. Within each experiment the time series is constant but can change between experiments. Especially between IV studies using different insulin analogs the time series vary a lot. However, for this work only human insulin is considered.

Fig.10 shows the glucose tracer and insulin IV curves. For insulin, there are two studies with a total of 23 experiments using human insulin. The tracer IV data sets contains one study with seven studies. They are plotted on a semi-log scale. Each measurement is displayed as a dot. To be able to follow the individual experiments better the dots are connected by lines. The lines however do not represent how the data behaves between the measurement points. It is to notice that the boli themselves are not displayed in the figures as they are given in 'pmol' whereas the measurements are given in 'pM'. Conversion between follows Eq.3.11. As the volume is unknown it is not possible to do

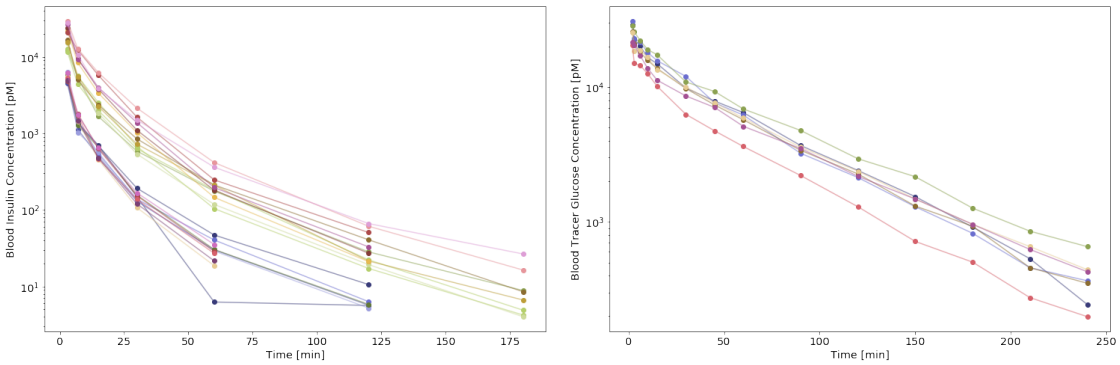

(a) Blood insulin IV curves

(b) Blood tracer glucose IV curves

Figure 10: IV curves for insulin (a) and tracer glucose (b). Each color represents one experiment, every dot is a measurement. The lines connecting the dots are only visual aids the follow one experiment. y-axis is on a logarithmic scale. Both display a multiphasic behaviour. Insulin (a) has high and low boli whereas tracer glucose only has one kind of boli.

the conversion and therefore not possible to display the boli in the figures.
The insulin IV curves are displayed in Fig.10a. From the curves it can be seen that there are two different regimes for the boli. The boli range from 351.6 to 1137.6 pmol/kg. Measurements were stopped when the insulin levels got too low. The experiments with low boli therefore contain less measurement points. The curves from the high and low bolus show a similar behaviour. From this it can be concluded that the insulin removal dynamics in this regime follow linearly with insulin bolus. The curves themselves do not follow a simple exponential but have a multiphasic decline. As opposed to Fig.7 these curves do not show a clear biphasic behaviour but more of a multiphasic behaviour with no clear exponential decays in any part of the slope.
In Fig.10b the tracer IV curves are shown. In contrast to the insulin IV data set the boli for the tracer experiments are close to each other. They range from 5759.8 to 6432.4 pmol/kg. All experiments have the same amount of measurements in them. Again the curves do not follow a single exponential decay but show a multiphasic behaviour. In these cases a biphasic decay seems to be the case. Similar to Fig.7 a first short steep decline is followed by a second more moderate decline.

4.2.2 Clamp Data

In the clamp data set three different kinds of clamp experiments are present; Euglycemic, Hyperglycemic and Hypoglycemic. The difference between the three experiments lies in the target glucose value. The target values are 5.7 mM, 9 mM and 3.5 mM, respectively. For this thesis only euglycemic experiments are of interest and hence all experiments have a target value of 5.7 mM. In addition to these three types there are also eleven different insulin analogs and human insulin used in the experiment. Again only the experiments using human insulin are of interest for this work. The clamp experiments containing tracer glucose were only performed as euglycemic experiments with human insulin.
Excluding the above mentioned studies as well as the two studies 'CLBR140201-3H test' and 'CLBR14-0201' leaves 227 clamp experiments in 11 studies. In addition there are 44 experiments including glucose tracer measurements from two different studies.

Each experiments contains a glucose and an insulin measurement. The glucose measurements starts at $t = -30$ min and is measured every 10 min for the whole duration of the experiment. The length of the experiments depends on the study with the shortest going 180 min and the longest going 300 min. Insulin is measured at different times depending on the study. The measurements are conducted in the interval [30, 300]. The glucose and insulin measurements are the same for the tracer experiments with the

addition of tracer measurements. Tracer glucose measurements only start at $t = 0$. In the tracer experiments movement data of the rats are also available. They are recorded every minute. The GIR starts at $t = 0$ and is recorded every 10 min. Between the time steps the GIR is assumed to be constant at the last known GIR level as no further information is available. During the experiment it is possible to adjust the GIR more frequently than every 10 min however glucose measurements are only performed at these time steps and changes of the GIR between them are unlikely to happen as there is no information to base the adjustment of the GIR on. In the glucose tracer experiments a glucose tracer bolus is injected at $t = -90$ and a constant tracer infusion rate is started. Once the GIR starts the glucose tracer infusion rates follows with a proportional factor of ~ 1000.

Fig.11 shows the output and input of an example experiment. To be able to fit all the information into one plot the insulin values are multiplied with a factor of 0.01.

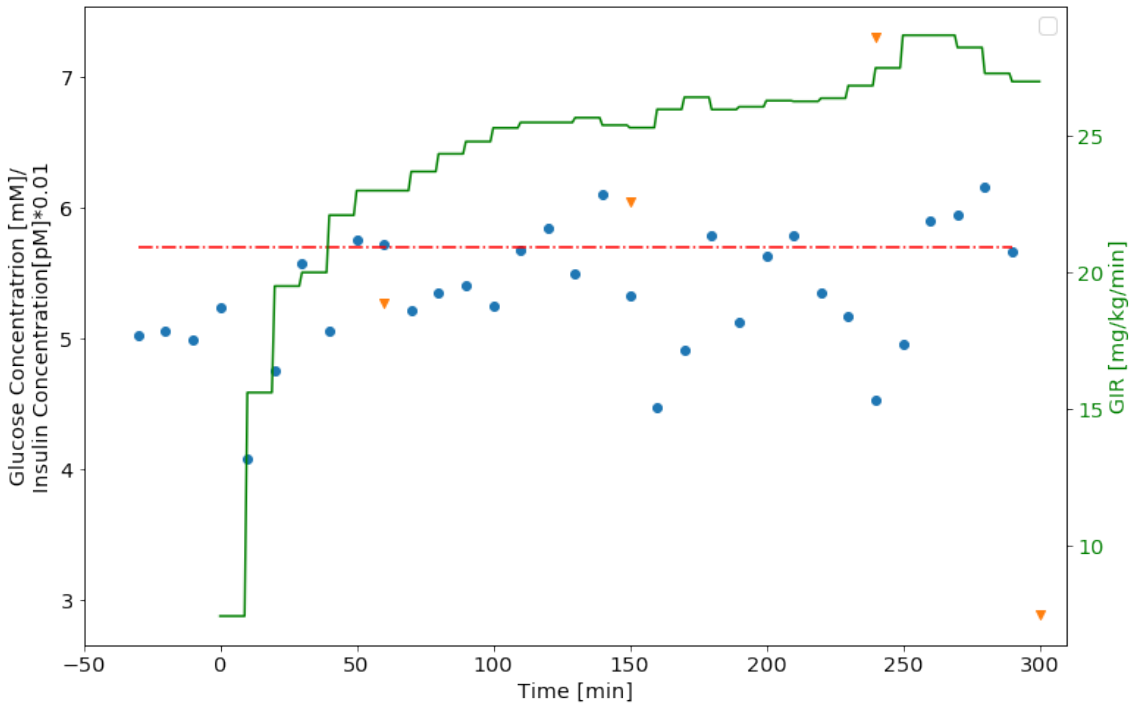

Figure 11: Data of a clamp experiment. The inputs and outputs of one example clamp experiment are shown. The left y-axis contains the glucose concentration in pM as well as the insulin concentration scaled by 0.01. The right y-axis contains the GIR. The x-axis is the time of the experiment. The blue dots show the glucose measurements, the orange triangles show the insulin measurements. The red dotted line is the target value for the glucose. The green line shows GIR over the course of the experiment.

As it is the goal of the euglycemic hyperinsulinemic clamp to get the blood glucose concentration as close as possible to the target value the glucose measurements are of little interest as they are kept in the same range for all experiments. Of more interest are the blood insulin concentrations as they are only regulated by the insulin infusion rate. With varying insulin infusion rate the blood insulin concentration is expected to vary as well. Another point of interest is the GIR. As the blood insulin concentration varies with the insulin infusion rate but the blood glucose concentration needs to be kept at the same level the GIR needs to compensate for that. The blood insulin concentration and the GIR should for theses reasons be able to provide the most information about the workings of the glucose insulin system.

In Fig.12 the blood insulin concentrations are shown at their times of measurement. The insulin concentration is plotted on a log scale. The insulin measurements are grouped by the insulin infusion rate used in the experiment. From the data in Fig.12 two features of the insulin concentrations can be seen. Firstly, the blood insulin concentrations increase with the insulin infusion rate and are spanning over multiple orders of magnitude. Secondly, the blood insulin concentrations seem to be in a steady state.

To further analyse the first point it is beneficial to look at the second point first. To determine if the blood insulin concentrations are in a steady state the coefficient of

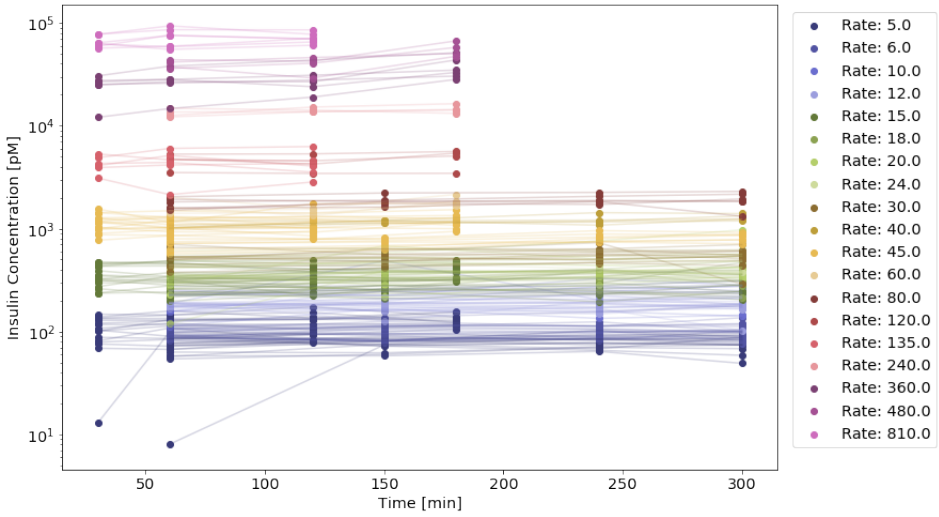

Figure 12: Insulin measurements. Each color represents one experiment, every dot is a measurement. The lines connecting the dots are only visual aids the follow one experiment. y-axis is on a logarithmic scale. x-axis gives the time of the measurements. Experiment duration varies between experiments. Insulin measurements seem almost constant over experiment duration.

Table 1: Mean, STD, median and interval of the coefficient of variation c_V for the insulin measurements.

	Mean μ	STD σ	Median	Interval
c_V	0.089	0.072	0.073	[0.007;0.575]

variation (CV) is calculated for every measurement. The CV is given by,

$$c_V = \frac{\sigma}{\mu}, \tag{4.1}$$

with σ being the standard deviation and μ being the mean.

Tab.1 shows the mean, the standard deviation, the median and the interval of the calculated CV's. With the mean, the STD and the median below 0.1 it shows that the measurements only deviate little from their mean. Hence, it is reasonable to assume that the blood insulin concentrations are in a steady state for the recorded measurement at all times. Small deviations from the steady state are to be expected in a complex biological system.

With the assumption that the blood insulin concentration is in a steady state at all measurement points it allows for a more convenient analysis of the properties of the data.

As mentioned above, the blood insulin concentration is dependent on the insulin infusion. Together with the assumption that the blood insulin concentration reaches a steady state the statement can be rephrased to: the steady state blood insulin concentration is dependent on the insulin infusion rate. In order to determine the kind of dependence Fig.13 shows the mean insulin steady state in dependence of the insulin infusion rate on a log-log scale. The relation seems to be almost linear. However, the steady state concentrations for high and low infusion values seem not to align. This behaviour is even more pronounced if the data is presented on a non-scale. It is therefore difficult to tell if the dependence is linear or non linear.

The assumption of the blood insulin concentration being in a steady state allows for further analysis. As described in Section 3.3.2, clearance gives the volume of blood that is cleared of the drug per unit time. In most cases, that would require a model. In steady state however, the removal of drug is given by the infusion rate, as they need to be of the same values. This allows for analysis of the insulin clearance in dependence of the blood insulin steady state concentration.

Fig. 14a shows the fractional blood insulin clearance as a function of the blood insulin concentration. The insulin clearance is, following Eq.3.16, defined as the insulin infusion

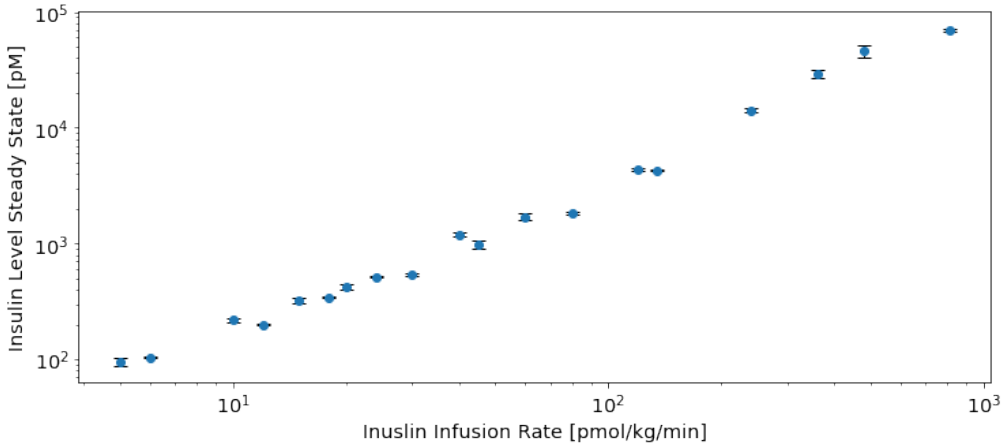

Figure 13: Insulin steady state in dependence of insulin infusion rate. The data is presented on a log-log scale with the error bars being the SEM. The mean insulin steady state concentration as a function of the insulin infusion rate. Both axis are on a log scale. A not quite linear relation between the two can be seen.

rate over the blood insulin steady state concentration. For each insulin infusion rate the average of the steady states have been taken. The error bars show the SEM. From the figure it can be seen, that the insulin clearance decreases with increasing blood insulin concentrations. Furthermore, the decrease of the clearance is non linear. In the beginning insulin clearance decreases with increasing blood insulin concentrations. With further increasing concentrations, however, the decrease of insulin clearance slows down until it seems to kind of reach a plateau in the end for high blood insulin concentrations. Besides the insulin infusion and the blood insulin concentration, the other measure of interest is the GIR as mentioned above. As the GIR is adjusted to keep the blood glucose concentrations at the target level, it should be affected by the changes in the insulin levels due to the different infusion rates. To investigate this relation, Fig.14b shows the mean GIR versus the blood insulin concentration steady state on a semi-log scale. Again, the average was taken over all measurements for one infusion rate. The error bars show the SEM. In Fig.14b it can be seen, that the mean GIR increases with blood insulin concentration for lower values. Around a blood insulin concentration of 100 pM the GIR reaches a plateau.

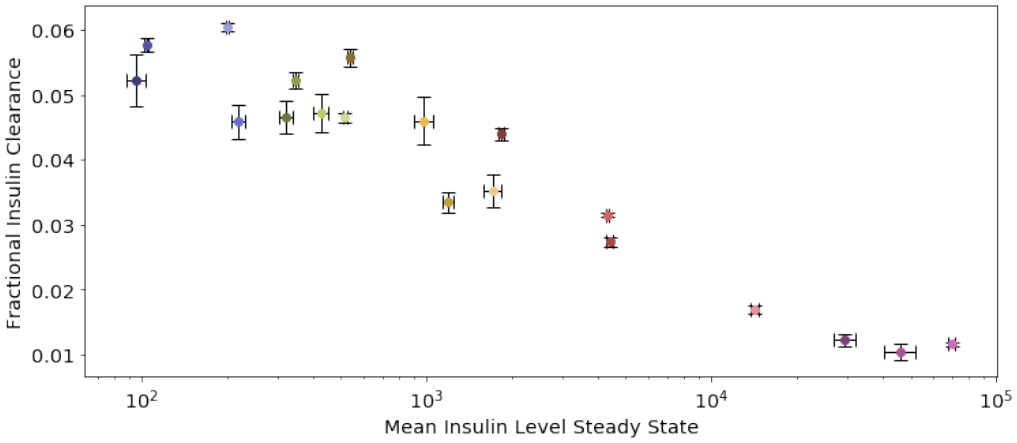

(a)

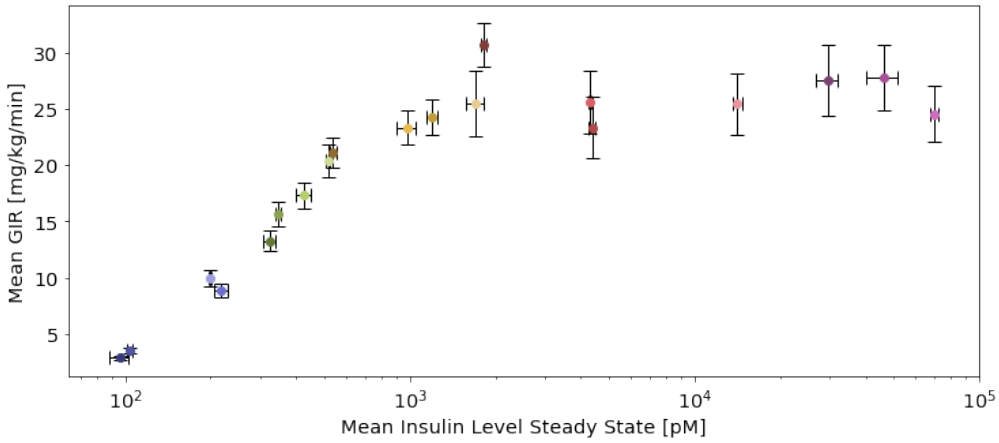

(b)

Figure 14: Analysis of the data. The error bars show the SEM. (a) shows the fractional insulin clearance as function of the mean insulin steady state. The colors indicate the insulin infusion rate. The x-axis is on a logarithmic scale. A non linear, saturable relation can be seen. (b) shows the mean GIR as a function of the mean insulin steady state. he colors indicate the insulin infusion rate. The x-axis is on a logarithmic scale. A saturation of the mean GIR can be seen.

5 Model of the Glucose Insulin System

The model proposed here consists of two two-compartment models that interact with each other. Models for the glucose insulin system using multi-compartment models that interact with each other have been proposed before by Dalla Man [18], Bergman [19] and Hovorak [20].

5.1 ODE Model

The model can be subdivided into two subsystems, a glucose subsystem and an insulin subsystem, that interact with each other. To support the determination of the parameters of the system a third subsystem can be introduced, a tracer glucose system. The system has no influence of the dynamics of the blood glucose and blood insulin concentrations. It can be influenced by either of the other two subsystems but does not do so in return. The tracer glucose system follows the dynamics of the glucose subsystem with the exception of not having any endogenous glucose production. Its only purpose is to help with the determination of parameters.
Fig.15 shows the scheme of the glucose insulin system. The upper part of the figure shows the insulin subsystem while to lower part shows the glucose subsystem. Processes that either increase or decrease the concentration in either compartment are shown by black arrows.

5.1.1 Insulin Subsystem

The insulin subsystem is given by a two-compartment model shown in the upper part of Fig.15. The two compartments in the model are the central C and peripheral P compartment. The central compartment describes the dynamics in the blood, extracellular fluids and highly perfused organs, the peripheral compartment on the other hand describes the dynamics in the periphery such as muscle mass and connective tissue. These description follow 3.3.4.

A two compartment model is used because it is known that insulin has biological functions in the blood circulation as well as in tissue, see Section 2.1.1. To further support a two compartment model, the IV curves in Fig.10a can be looked at. They display mul-

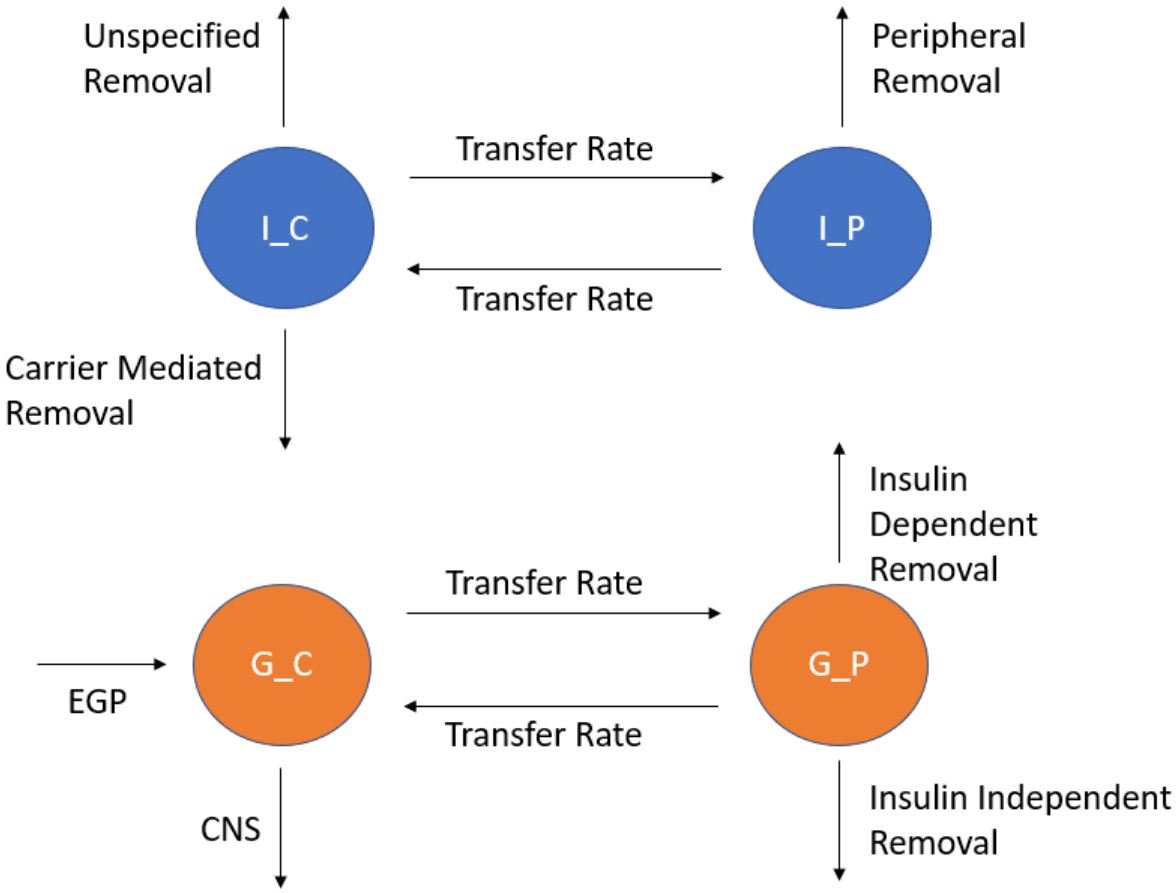

Figure 15: Schematic presentation of the insulin glucose system. The upper part of the figure shows the two-compartment model of the insulin subsystem, the lower part shows the two-compartment model of the glucose subsystem. Arrows indicate movement of insulin/glucose from and to compartments.

tiphasic behaviour. To be able to describe these dynamics a model containing multiple compartment is necessary.

The equations describing the model are given by,

$$\frac{dI_C}{dt} = k_{21}I_P - k_{12}I_C - n_{IC}I_C\left(0.8\frac{k_{IC}V_{IC}}{k_{IC}V_{IC}+I_C} + 0.2\right) \tag{5.1a}$$

$$\frac{dI_P}{dt} = -k_{21}I_P + k_{12}I_C - n_{IP}I_P\frac{k_{IP}V_{IP}}{k_{IP}V_{IP}+I_P} \tag{5.1b}$$

$$[I_j] = \frac{I_j}{V_{Gj}}, \quad \text{for } j = C, P. \tag{5.1c}$$

I_C, I_P, $[I_C]$ and $[I_P]$ are the amounts and concentrations of exogenous insulin in the central and peripheral compartment, respectively. The parameters k_{21} and k_{12} are transfer rates between the two compartments. n_C and n_P are removal rate parameters in their respective compartments. n_C is the sum of the linear removal rate parameter and the maximum elimination rate of the Michaelis-Menten term. n_P on the other hand is only the maximum elimination rate of the Michaelis-Menten term. The parameter k_{IC} and k_{IP} are Michaelis-Menten constants. V_{IC} and V_{IP} give the apparent volume of distribution of the central and peripheral compartment.

The removal term in Eq.5.1a consists of two separated processes, a linear removal term and non-linear Michaelis-Menten removal term. The use of this structure is motivated by Fig.14a. The figure shows the clearance of insulin as a function of blood insulin concentration at steady state. The clearance shows a non linear behaviour. For lower insulin levels the clearance follows a linear relation. A linear removal rate for this range would be sufficient. Models such as Hovorak [20] use a linear removal rate from their insulin compartments. For higher insulin values, however, a linear removal rate is not sufficient anymore as can be seen in Fig.14a. A combination of the two removal rates, a non-linear Michaelis-Menten and a linear removal term, is proposed in this model. Neither of them on their own should be able to describe the dynamics that can be seen as a singular Michaelis-Menten term would not be able to describe the linear slope in the beginning as well as the non zero clearance at the saturated levels. A combination of a linear clearance and non linear clearance, however, could be able to so. A biological interpretation of the two terms is given by a receptor mediated processes for the Michaelis-Menten term and some unspecific clearance of multiple processes in the central compartment for the linear term.

As the peripheral compartment is only a theoretical compartment is it not possible to have any measurements that could help with determining its dynamics. Models such as Dalla Man [18] and Bergman [19] use a linear removal term. However, since the data suggested a saturabel process the central compartment a similar process will be assumed

for the peripheral compartment. The removal of insulin in the central compartment is therefore described by non linear Michaelis-Menten dynamics.
The insulin subsystem does not contain an insulin secretion term as the insulin dynamics described in this model refer to the exogenous injected insulin. Since the exogenous insulin differs from the endogenously produced insulin of the rat, the only the source of insulin in the model is the infusion rate. The total amount of insulin in either compartment is therefore not only given by the values from the model but also from the endogenous insulin present in the model. Any insulin and glucose dynamics should therefore not only depend on the insulin amounts given by Eq.5.1 but by the total amount of insulin in these compartments $I_{j,total}$. However, as any dynamics in the insulin compartment only start when exogenous insulin is infused and as the amount of infused exogenous insulin is large compared to the amount of endogenous insulin, the simplification can be made that only the exogenous insulin determines the dynamics of the exogenous insulin. For glucose on the other hand, such an assumption can not be made, as some measurements of glucose and tracer glucose occur when no external insulin has been injected. Therefore, glucose depends on the total amount of insulin in the compartments $I_{j,total}$. In order to find the total amount of insulin, the endogenous blood insulin concentration I_{endo} is required. As the rats are in a fasting state and no exogenous glucose is injected before any exogenous insulin is injected it is assumed that the endogenous insulin level will never rise above basal levels I_{basal}. In addition to that it is assumed that the amount of endogenous insulin will decrease linearly with the amount of exogenous insulin as any endogenous insulin production will be suppressed and the endogenous insulin will be replaced with exogenous insulin. This yields following equations for the endogenous insulin amounts,

$$I_{j,endo} = \max(I_{j,basal} - I_j), \tag{5.2}$$

with $j = C, P$ for the respective compartments.
The total insulin levels for the central and peripheral compartment are then given by the sum of the endogenous and the exogenous insulin levels,

$$I_{j,total} = I_j + I_{j,endo}. \tag{5.3}$$

Eq.5.1c follows the concept of the apparent volume of distribution described earlier. Through substitution of Eq.5.1c into Eq.5.1a and Eq.5.1b it makes it possible to have the model in terms of concentrations or amounts.

5.1.2 Glucose Subsystem

To have a two-compartment model for glucose follows the same line of argumentation as for insulin. Mechanisms of glucose in the central regions as well as in peripheral tissue are known, see Section 2.1.2. From the IV curves in Fig.10b a non biphasic behaviour can be observed, further supporting the usage of a multi-compartment model.
The two-compartment model consists of a central C and a peripheral P compartment. Their respective contents are the same as described in the insulin subsystem chapter above.
The structure of the model is displayed in the lower part of Fig.15. The equations for the model are given by,

$$\frac{dG_C}{dt} = EGP - k_1 G_C + k_2 G_P - F_{CNS}, \tag{5.4a}$$

$$\frac{dG_P}{dt} = k_1 G_C - k_2 G_P - n_{GP} G_P \frac{G_P}{k_{GP} V_{GP} + G_P} \frac{I_{P,total}}{k_{IP} V_{IP} + I_{P,total}}, \tag{5.4b}$$

$$[G_j] = \frac{G_j}{V_{Gj}}, \quad \text{for } j = C, P, \tag{5.4c}$$

with G_C, G_P, $[G_P]$ and $[G_C]$ being the glucose amounts and concentrations in the central and peripheral compartment. k_1 and k_2 are the transfer rates between the central and the peripheral compartment, V_{GC} and V_{GP} are the apparent volumes of distribution of the central and peripheral compartment, EGP is the endogenous glucose production, F_{CNS} is the insulin independent glucose uptake of the central nervous system, n_{GP} is the removal rate parameter in the peripheral compartment, k_{GP} and k_{IP} are Michaelis-Menten constants for a glucose dependence and an insulin dependence in the peripheral compartment, respectively and $I_{P,total}$ is the total insulin concentration in the peripheral compartment.
The EGP is given as a function of the glucose and total insulin concentration in the central compartment,

$$EPG = \max(k_{EGP,0} - k_{EGP,G} G_C - k_{EGP,I} I_{C,total}, 0) \tag{5.5}$$

with $k_{EGP,0}$ being the endogenous production rate of glucose for zero glucose and insulin and $k_{EGP,G}$ and $k_{EGP,I}$ being the rate parameters for the suppression of glucose production for glucose and insulin.
Glucose G_C and insulin $I_{C,total}$ in the central compartment suppress the production of the endogenous glucose in a linear way. This description of the EGP follows the idea introduced in [21]. While the models in [21] are much more sophisticated, it is not possible to follow these as the required data is not given. Therefore, more simple version of

the EGP is used in this model.
The insulin independent glucose uptake of the central nervous system F_{CNS} is assumed to be constant for all levels of blood glucose and insulin since the brain uses mainly GLUT1 as its transporter protein. With the presence of GLUT1 being not dependent on the insulin or glucose concentration a constant term was chosen.
The removal term in Eq.5.4b describes the insulin dependent and the glucose dependent removal of glucose from the peripheral compartment in one non linear term. The term is composed of two non linear Michaelis-Menten terms describing the effects of the blood glucose concentration and the total blood insulin concentration.
The insulin dependent removal of glucose is mainly driven by GLUT4 as explained in Section 2.1.1. It follows that the insulin dependent glucose uptake is dependent on the number of specific insulin receptors insulin can bind to as well as the number of GLUT4 transporters available for glucose uptake. As the binding of insulin to its receptors is the cause for GLUT4 transporters to be released a proportionality between the two can be expected. The GLUT4 concentration is therefore be approximated by the insulin concentration in this model. The non linearity originates from the amount of receptors and GLUT4 transporters available as there is only a finite amount. To reduce the amount of parameters in the model an assumption is made. As the insulin is binding to its receptors it is removed from the system. The non linearity of the removal of insulin in the insulin subsystem could therefore be related with the release of the GLUT4 transporters. Based on this assumption, the Michaelis-Menten constant from the insulin removal in the insulin subsystem will be used for the insulin dependent removal of glucose in the glucose subsystem.
Fig.14b. shows the mean GIR in dependence of the mean insulin steady state. It can be seen that the GIR reaches a plateau even though the insulin steady state values increase further. The insulin dependent glucose removal is therefore given by Michaelis-Menten dynamics in dependence of the insulin concentration in the periphery,

$$U_{IDG} = V_{IDG} \frac{I_{P,total}}{k_{IP} V_{IP} + I_{P,total}}, \tag{5.6}$$

with $I_{P,total}$, k_{IP} and V_{IP} as introduced above and V_{IDG} being the maximum elimination rate of the insulin dependent glucose removal.
The glucose dependent glucose part of the glucose removal term U_{GDG} also follows non linear Michaelis-Menten dynamics. Glucose uptake of cells is in many cases a carrier mediated process such as glucose transporter protein. As it is the case with any carrier mediated process a saturation effect will occur once the amount of carrier is exhausted.

A Michaelis-Menten removal term is therefore used. It is given by

$$U_{GDG} = V_{GDG} G_P \frac{k_{GP} V_{GP}}{k_{GP} V_{GP} + G_P}, \tag{5.7}$$

with G_P, k_{GP} and V_{GP} introduced as above and V_{GDG} being the maximum elimination rate of the glucose dependent glucose removal.
The model for the tracer glucose can be found in Appendix A

5.2 Model Complexitiy Reduction

It proved to be not possible to estimate the parameters of the previous two-compartment model. The amount of parameters in combination with the quality of the data present lead to a situation where it was not possible to determine the parameters of the model in way that would lead towards the goal of having a distribution of all the parameters based

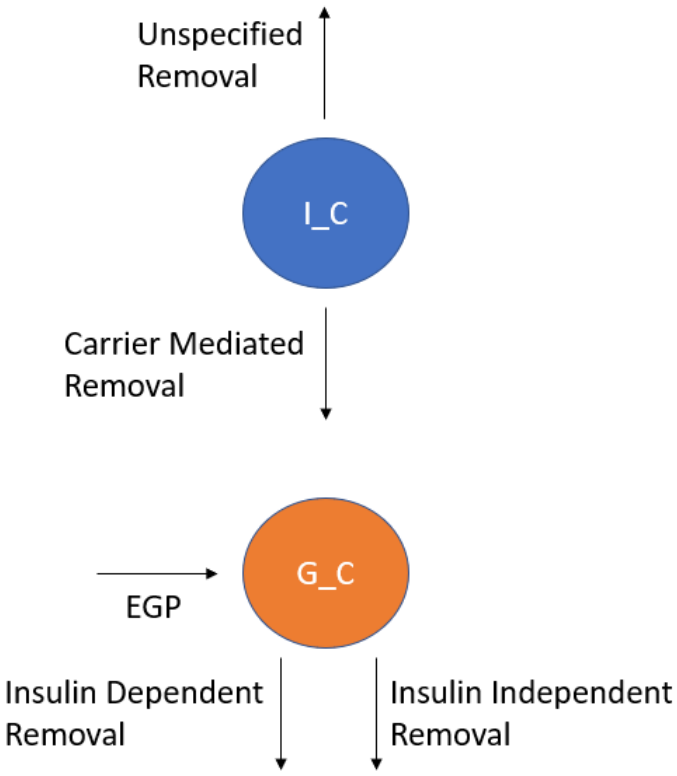

Figure 16: Schematic presentation of the reduced insulin glucose system. The upper part of the figure shows the one-compartment model of the insulin subsystem, the lower part shows the one-compartment model of the glucose subsystem. Arrows indicate movement of insulin/glucose from and to compartments.

on the individual fits using Bayesian inference with Stan. The amount of parameter and the quality of the data is not necessarily the reason for our failure. Problems with the Bayesian inference using Stand occurred during that period. Further information about that can be found in Appendix B.
The decision was made to reduce the complexity of the model rather than change the method of determining the parameters.
To reduce the model in complexity, a different approach to the problem was taken. Models such as Dalla Man [18], Bergman [19] and Hovorak [20] are trying to describe the insulin-glucose system as accurate as possible and as the insulin-glucose system is complex these models also tend to be complex. The downside to that complexity is that the amount of parameters that need to be estimated.
In this chapter a more simplistic model is introduced with the knowledge that it will not be able to describe all the dynamics of the insulin glucose system but which should be capable of modeling the euglycemic hyperinsulinemic clamp experiments which was the goal of the thesis to begin with. Similar approaches have been done in [22] and [23].

5.3 ODE Model

Similar to the previous model this model can be divided into two subsystems, an insulin subsystem and a glucose subsystem with a tracer subsystem that follows the glucose subsystem closely. The structure of the whole system is is shown in Fig.16.

5.3.1 Insulin Subsystem

The structure of the insulin subsystem can be seen in the upper part of Fig.16. The biggest difference between this model and the previous model is that the insulin subsystem only consists of one compartment instead of two. It is also notable that the two compartments have not been merged but that the peripheral compartment from the previous model simply got removed yielding the insulin subsystem used in this model,

$$\frac{dI}{dt} = -k_{Ie} I \left(0.8 \frac{k_I V_I}{k_I V_I + I} + 0.2 \right) \tag{5.8a}$$

$$[I] = \frac{I}{V_I}, \tag{5.8b}$$

with I, $[I]$ being the insulin amount in the blood and the blood insulin concentration, respectively, k_{Ie} being the removal rate, k_I being the Michaelis-Menten constant and V_I being the apparent volume of distribution of the insulin system.
The argumentation for the terms used in the equation is the same as in Section 5.1.1 and is therefore not repeated here.

Reducing the number of compartments from two to one will affect the ability of the model to capture some of the dynamics involved in the glucose insulin system. As said in Section 5.1.1 the insulin IV curves show a distinct multiphasic behaviour. To be able to describe such behaviour at least a two-compartment model is necessary. It follows that Eq.5.8 will not be able to describe the insulin IV data. In the context of the euglycemic hyperinsulinemic clamp experiment this is however not too important as the insulin is given in constant rate over the whole experiment as opposed to a single bolus in the IV experiment. The steady state behaviour between the two models is similar with the only difference being the additional removal term in the periphery in Eq.5.1b. The big difference in the modeling of the euglycemic hyperinsulinemic clamp experiment would be the dynamics of how the steady state is reached. However as it can be seen from Fig.12 the blood insulin concentration has already reached its steady state by the time of the first measurement and remains at it for the duration of the experiment. Therefore the one-compartment insulin system should suffice in describing the insulin dynamics in the euglycemic hyperinsulinemic clamp experiment.
Similar to the model introduced in Section 5 the insulin considered in this model only refers to the exogenous insulin. The total amount of insulin in the blood I_T is, as described above, the sum of the the amount of endogenous and exogenous insulin in the blood. The modeling of the endogenous insulin in this model is given by,

$$I_{endo} = \max(I_{basal} - I) \tag{5.9}$$

$$I_{total} = I + I_{endo}, \tag{5.10}$$

with I_{basal} being the amount of endogenous insulin in the blood at basal levels of glucose and I_{endo} being the amount of endogenous insulin levels in the blood at any time.

5.3.2 Glucose Subsystem

The glucose subsystem is likewise reduced to a one-compartment model. The model structure can be seen in the lower part of Fig.15. In contrast to the insulin subsystem which uses the central compartment from the previous model the glucose subsystem in this model uses some features from both, the central and the peripheral, compartments from the previous model. The model is given by,

$$\frac{dG}{dt} = EGP - k_{Ge}\frac{G}{k_G V_G + G}\frac{I_{total}}{k_I V_I + I_{total}} \tag{5.11a}$$

$$[G] = \frac{G}{V_G}, \tag{5.11b}$$

with G, $[G]$ being the amount of glucose in the blood and the blood glucose concentration, respectively, EGP being the endogenous glucose production, k_{Ge} being the removal rate parameter, k_G and k_I being Michaelis-Menten constants for the insulin independent and insulin dependent removal of glucose, respectively, I_{total} being the total amount of insulin in the blood and V_G, V_I being the apparent volumes of distribution for the glucose and the insulin system, respectively.
The EGP again is a function of the amount of glucose and insulin in the blood. It is given by,

$$EGP = \max(k_{EGP,0} - k_{EGP,G}G - k_{EGP,I}I, 0), \tag{5.12}$$

with $k_{EGP,0}$ being the endogenous production rate of glucose for zero glucose and insulin and $k_{EGP,G}$ and $k_{EGP,I}$ being the rate parameters for the suppression of glucose production for glucose and insulin. As the terms used in this model are similar to the ones used in the previous model they will not be explained again. For a detailed description of the terms see Section 5.1.2.
Merging the two compartments from the previous model will diminish the models ability to describe all the glucose dynamics. As in the case of insulin, this glucose model will not be able to describe the glucose IV curves as they also show a multiphasic behaviour that can not be recreated in a one-compartment model. However, this more simple model should be able to describe the dynamics of the euglycemic hyperinsulinemic clamp experiment regardless. As can be seen in Fig.10b the first phase of the IV curves only takes a short time. After only a few minutes the second phase, the removal phase, sets in. It follows therefore that glucose equilibrates fast between the central circulation and the tissue. Once this equilibrium state is reached the two-compartment model behaves like a one-compartment model. This, however, applies mainly for IV studies as there is no further input after the injection but the glucose model has a time varying input in the GIR. Still as the time to reach an equilibrium state is quite low the one-compartment model should fulfill the requirements to model the euglycemic hyperinsulinemic clamp experiment.

5.4 Parameter Estimation and Discussion

The full model is given by Eq.5.8, 5.9, 5.10, 5.11, 5.12 and A.2. It contains ten parameters that need to be estimated.
Again the amount of parameters does not allow to fit everything at the same time. The fitting process needs to be separated into different steps in an iterative way to determine

the parameters. Parameters determined in previous fit will be used to determine the next parameters.
In the first step I_{basal} will be determined. To do so, the GIR in steady state together with the insulin in steady state is used to extrapolate the insulin level for $GIR = 0$. This value is then taken as I_{basal}. In the second step the insulin parameter will be determined as the insulin subsystem is only insulin dependent. Initially the insulin values from the tracer data set will be used due to the fact that they only contain two different studies with a total of three different infusion rates. The knowledge about the range of the parameter values will then be used to fit the insulin data from the clamp experiments which contains a much larger range of insulin infusion. In the next step the tracer data is fitted. The tracer model is fitted ahead of the glucose model as it contains the same parameters but does not have the EGP term. The parameters determined from the tracer data can then be used to fit glucose model first with the tracer data set and then with clamp data set. The parameters known from the tracer model are fixed.

5.4.1 Basal Insulin

To determine the endogenous insulin blood concentration I_{basal} the clamp data set is used. As there are no measurements of the blood insulin concentration for no GIR the value needs to be determined by extrapolation. The steady state values of the GIR and the blood insulin measurements are used for that. Since the blood insulin reaches its steady state value already before the first measurement it does not need to be taken into to consideration. The GIR however is changed a lot during the experiment only during the last hour is it supposed to reach a steady state. Therefore, only the last hour is taken into consideration when determining the steady state values of the GIR and blood insulin concentrations. If the mean glucose value in the last hour was above 6 the experiment got excluded as in that case the glucose concentration would have been significant above the target and GIR would have been reduced significantly in respond to that. In the last step and experiments with GIR values above 5 are excluded to be localized to allow for a simple linear regression,

$$y \sim \mathcal{N}(\alpha + \beta \cdot x, \sigma^2), \tag{5.13}$$

where y is the insulin steady state value and x is the GIR value.
The result of the linear regression can be seen in Fig.17. It is visible that the fit has some uncertainty because the values are spread pretty far. The general trend has been captured regardless of that. The fit values are given in Tab.2. α corresponds to the parameter I_{basal} in our model.

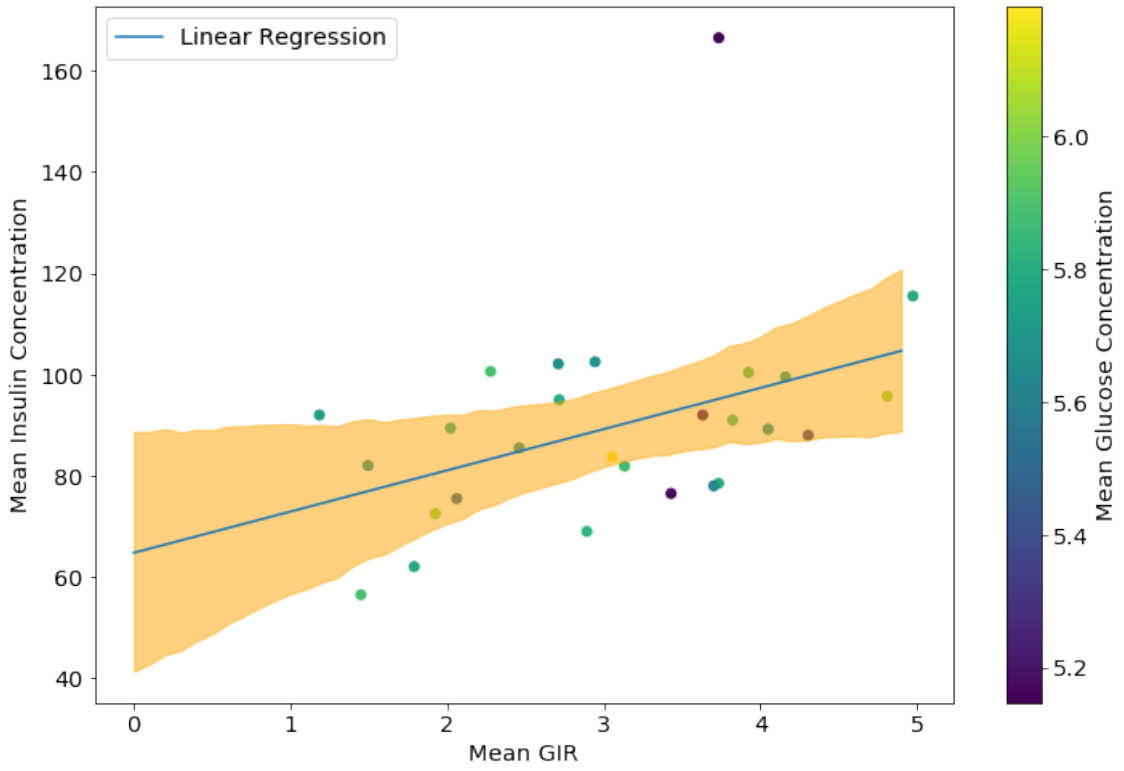

Figure 17: Basal insulin estimation. The basal insulin concentration is estimated by a linear regression of the mean insulin concentration as a function of the mean GIR. Only experiments with a mean glucose concentration below 6 mM a mean GIR below 5 mg/kg/min are considered. The linear regression is shown by the blue line. The orange area indicates the 95% confidence interval.

Table 2: Mean values with their respective STD for the parameters of the linear regression

	Mean	STD
α	64.272	12.216
β	19.848	3.056
σ	8.307	3.838

5.4.2 Insulin

The ODE model that is to fit the insulin data from the tracer data set is given by Eq.5.8 with the addition of the infusion rate X_I,

$$\frac{dI}{dt} = -k_{Ie}I\left(0.8\frac{k_I V_I}{k_I V_I + I} + 0.2\right) + X_I \tag{5.14a}$$

$$[I] = \frac{I}{V_I} \tag{5.14b}$$

$$I(0) = 0. \tag{5.14c}$$

The above model has been fitted using Bayesian inference in Stan. The statistical model used is given by,

$$y_{ij} \sim \mathcal{N}\left(f(t_{ij};\theta_i), \sigma^2\right), \tag{5.15a}$$

$$\theta_{ik} \underset{\text{i.i.d.}}{\sim} \text{Lognormal}\left(\log(\beta_k), \omega_k^2\right), \tag{5.15b}$$

with f being the numerical solution of the model integrated with a fourth and fifth order Runge-Kutta method, $\theta = (k_{Ie}, k_I, V_I)$, β_j and ω_j being the parameters defining the prior distribution. A log-normal distribution for the parameters was used in order to restrict the parameter space to only positive values. Due to small range of insulin steady states a constant error model was implemented. The values for β_j and ω_j are given in Tab.3. To give the algorithm good starting parameters an initial scan of the parameter space was performed manually. The values that resulted in the best fit are the ones reported in Tab.3 as the mean value of the prior distribution.
A total of four chains were run for the fit. Each chain containing a total of 2000 iterations with a burn-in period of 1000 iterations. The `adapt_delta` was set to 0.8. To keep the numbers of iteration low but still enable a sample with reduced auto correlation a thinning of two was used.

The resulting fit values are shown in Tab.3. Fig.18 shows four mean trajectories with their corresponding 95% confidence interval representing each insulin infusion rate (6, 12, 18) at least once. The shown examples fit the data in a good way. As discuss in Section 4.2, insulin is at all measurement points in a steady state. The is fit able capture that behaviour.

Before checking the model for validity, however the Bayesian inference itself should be inspected. The trace plots in the right hand side of Fig.19. shows the trajectories for the individual chains by parameters. From the figure it can be seen that during the sampling process no divergences happened as these would be indicated by black vertical lines, and that the chains are mixed, the chains all end up in the same region in the

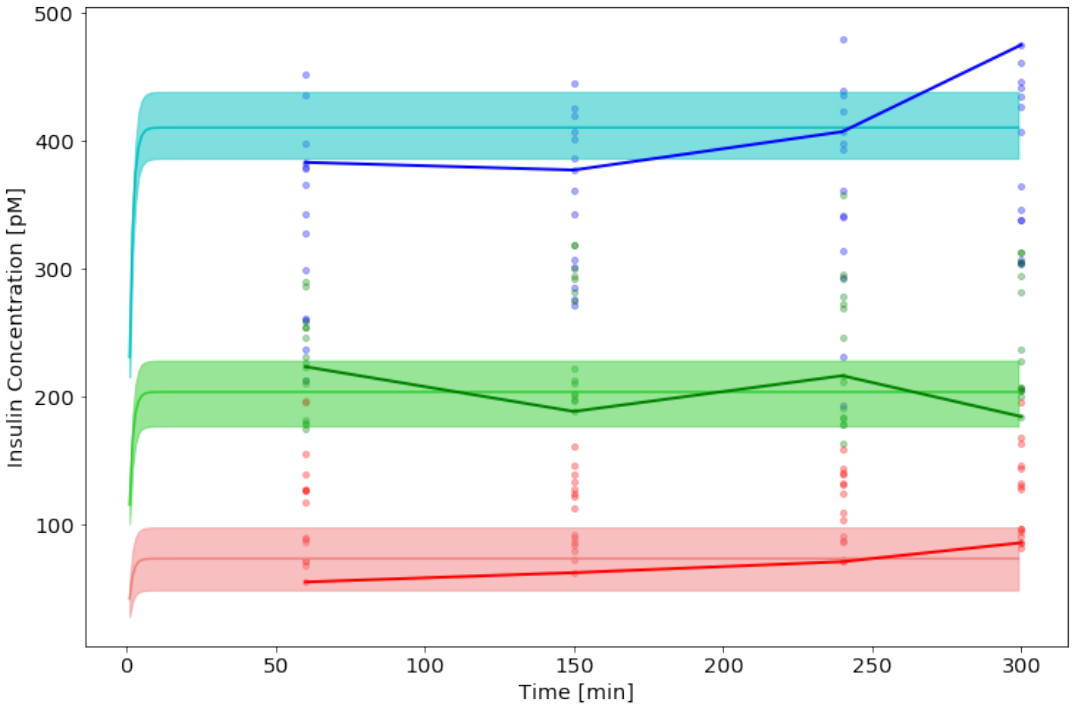

Figure 18: Insulin fit tracer data set. Three example measurements with their respective fits are shown for the three different insulin infusion rates: 6 (red), 12 (green) and 18 (blue). The fits are the lighter colors and are shown with their 95% confidence interval. The fitted measurement are given by dark colored lines. Dots in the respective colors show the remaining measurements with the respective insulin infusion rate.

parameter space despite having different starting conditions. Looking at the traces from V_I however it can be seen that the traces are not covering the area 0.6. This can be made more visible by plotting the histograms of the values the individual chains take.

Table 3: Priors and posteriors for the insulin fits of the the tracer data set. Prior values are given before the are log transformed. Posteriors shown are the mean and STD over the mean of all experiments

	Priors		Posteriors	
	Mean	STD	Mean	STD
k_{Ie}	8.5e−01	1e−01	8.44e−01	2.99e−04
V_I	5.6e−02	5e−02	6.42e−02	1.44e−02
k_I	1.9e+04	5e+03	1.84e+04	2.98e+01
σ	5e+01	2e+01	2.76e+01	1.71e+00

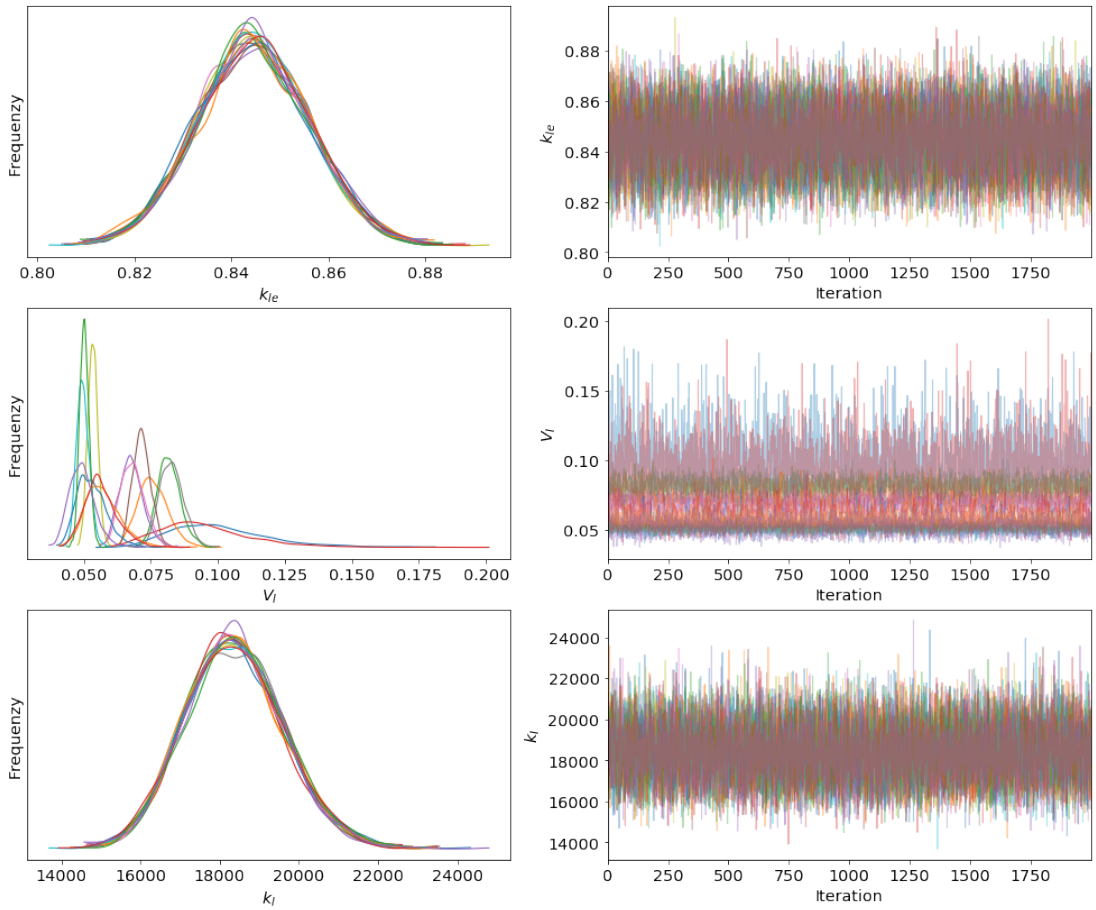

Figure 19: Chains of the Bayesian inference for the parameters. The chains of the three parameter k_{Ie}, V_I and k_I that were estimated are shown from top to bottom. On the right hand side the values the individual chains took during the Bayesian inference are displayed. The left hand side shows smoothed histograms of these values. For clarity reasons only every third fit is shown. The fits shown are representative for all fits.

They are shown on the left hand side of Fig.19. With the traces presented like that it is quite clear that V_I the individual distributions of V_I are not located around the same values. From the figure it seems as if there are two different parameter values that the parameters take. The individual curves, however, do not display a bimodal behaviour. The individual parameters of k_{Ie} and k_I also both follow monomodal distributions but mean values lie closer to each other.

For the posterior distribution of the parameters of the individuals a monomodal distribution that has a similar mean and variance as the other individuals would have been expected. Rat to rat variance is expected which is why a hierarchical model was used in the first place. The underlying assumption was however that the parameters from

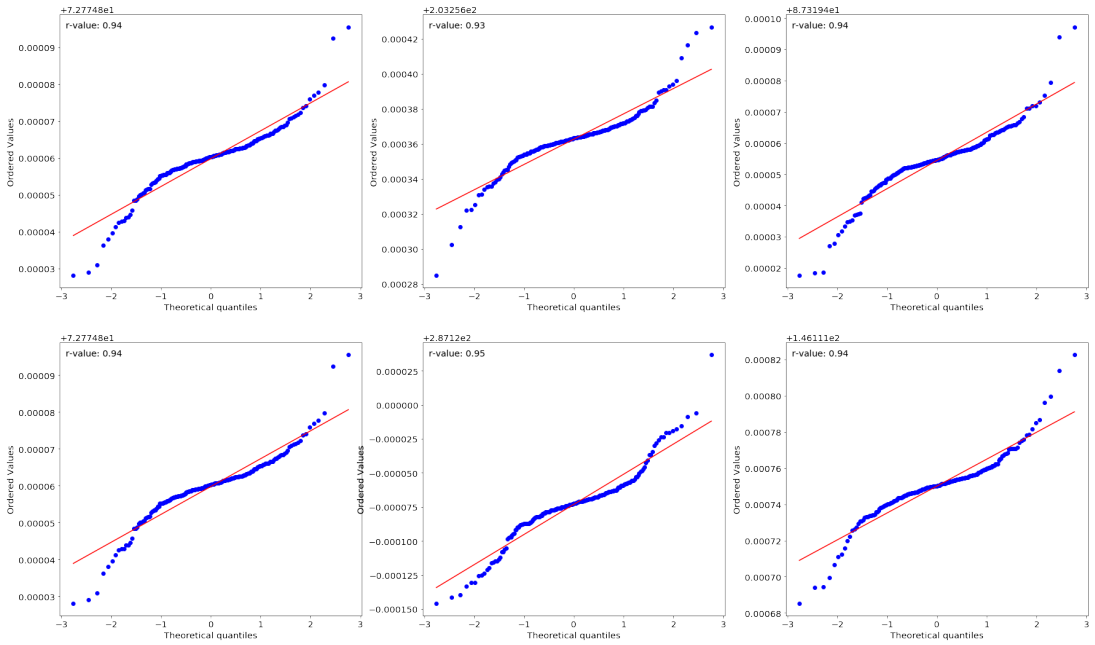

Figure 20: QQ-Plot for insulin fits. Six example QQ-plots from the insulin fit are shown with a linear regression fit. The y-axis shows the quantiles of the fits starting at the first measurement point at $t = 60$. The x-axis shows theoretical qunatiles of a normal distribution with mean zero and STD 1. The linear regression is given by the blue line. The respective r-value of the linear regression is displayed in the upper left corner of each plot.

the individual rats would form a monomodal distribution as there are no systematic differences between the rats. This is represented by the lognormal-distribution that is used as a prior distribution. The spread of the individual parameters for V_I that occurs in this case is unexpected. Further analysis showed, that the parameter center around two values. The rats of the two values are from different studies. In Fig.19 this split can be observed. Why this split happens is unknown as the experiments should follow the same structures as discussed in Section 4.2. A possibility would be that the rats were provided by different vendors and therefore have some differences between them.
To check for the validity of the statistical model QQ-plots and their respective r values can be used. This analysis is inspired by the analysis of the statistical model in [23]. Fig.20 shows the QQ-plots of the first and last four experiments as an example. By looking at the plots no immediate errors are visible. For a more quantitative measure the r values of the linear regression are used. The values all are in the interval $[0.973, 0.722]$ with a mean value of 0.867. These values indicate that the model used is valid.

With the validity of the model for the insulin data in the tracer data set shown the

model will be applied to the insulin data in the clamp data set. The difference between the two data sets, as pointed out earlier, is the range of the insulin infusion. With the validity of the model confirmed for the lower, more natural insulin infusion ranges the data set containing high insulin infusion rates will tested.
For the fit of the insulin data in the clamp data set the model in Eq.5.14 will be used. The associated statistical model for the Bayesian inference follows Eq.5.15 closely and is given by,

$$y_{ij} \sim \mathcal{N}\left(f(t_{ij};\theta_i), f(t_{ij};\theta_i)\sigma^2\right) \tag{5.16a}$$

$$\theta_{ik} \underset{\text{i.i.d.}}{\sim} \text{Lognormal}\left(\log(\beta_k), \omega_k^2\right), \tag{5.16b}$$

with the variables and parameters following the description above.

The difference between the two statistical models is, that a proportional error model is used instead of a constant error. This is due to the fact that through the large range of insulin infusion rates the resulting blood insulin steady states multiple orders of magnitudes span. To have a relevant error for all fits it is therefore not possible to use a constant error as in the previous model but to use a proportional error model.
The same settings for the sampling were used as for the clamp data set. The mean of the previously determined parameters were used to define the prior distribution. Initially also the standard deviation from the previous fit were used. However, the accuracy of the resulting fits was low and in respond to that the standard deviation was adjusted. The reported values in Tab.4 show all the values used for the sampling.

In Fig.21 example fits for high and low infusion rates are shown. Looking at the fits for the low insulin infusion rates it seems like they are fitted well. This was to be expected as the insulin infusion rates in the previous data set covered a similar range. The high insulin infusion rates are of more interest as they are affected by the non linearity that

Table 4: Priors and posteriors for the insulin fits of the clamp data set. Prior values are given before the are log transformed. Posteriors shown are the mean and STD over the mean of all experiments

	Priors		Posteriors	
	Mean	STD	Mean	STD
k_{Ie}	8.36e−01	1e−01	8.28e−01	1.10e−03
V_I	1.04e−01	5e−02	6.32e−01	1.60e−02
k_I	1.8e+04	2e+03	1.78e+04	8.30e+00
σ	8e−02	1e−02	1.49e−01	4.34e−03

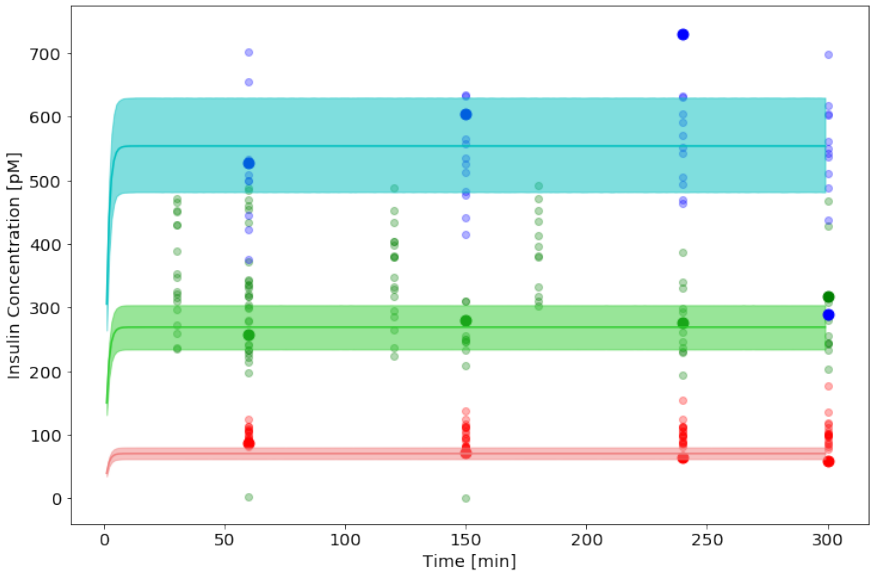

(a) The insulin infusion rates for red, green and blue are 5, 15, 30, respectively.

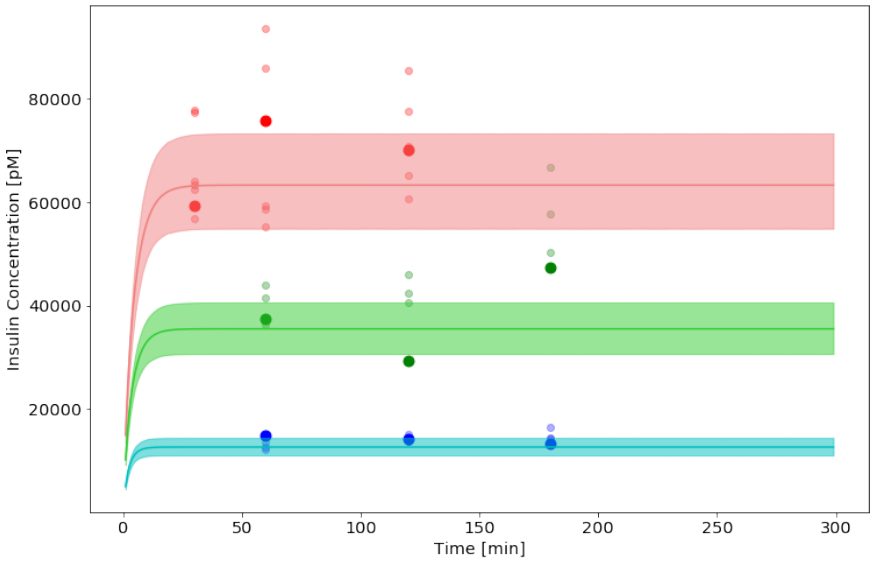

(b) The insulin infusion rates for red, green and blue are 810, 480, 240, respectively.

Figure 21: Insulin fit of high and low insulin infusion rates. Three exemplary insulin fits for low (a) and high (b) insulin values are shown. The colors in the plots indicate the insulin infusion rate. The measurements fitted are indicated by big dots. Other measurements of the same infusion rate are shown as smaller dots of the same color. The fits are shown in lighter colors with the 95% confidence interval. (a) The insulin infusion rates for red, green and blue are 5, 15, 30, respectively.

can be seen in Fig.13 while the low infusion rates can be modeled as linear. From the fits in Fig.21 it can be seen that the model seem to be able to capture the steady states of the high insulin infusion quite good. Though through variation in the data not all data points are within the 95% HDI interval it however seems as if the average falls within it. The results suggest that the proposed model is capable of describing the insulin steady states for low and very high insulin infusion rates.

Following along the lines of the previous analysis it is wise the see how Bayesian inference performed. Thus the trace plots of the parameters are explored first. They are shown in Fig.22. The first observation that can be made is that there are again no divergences. There is however a pretty big difference between the trace plot of V_I and the

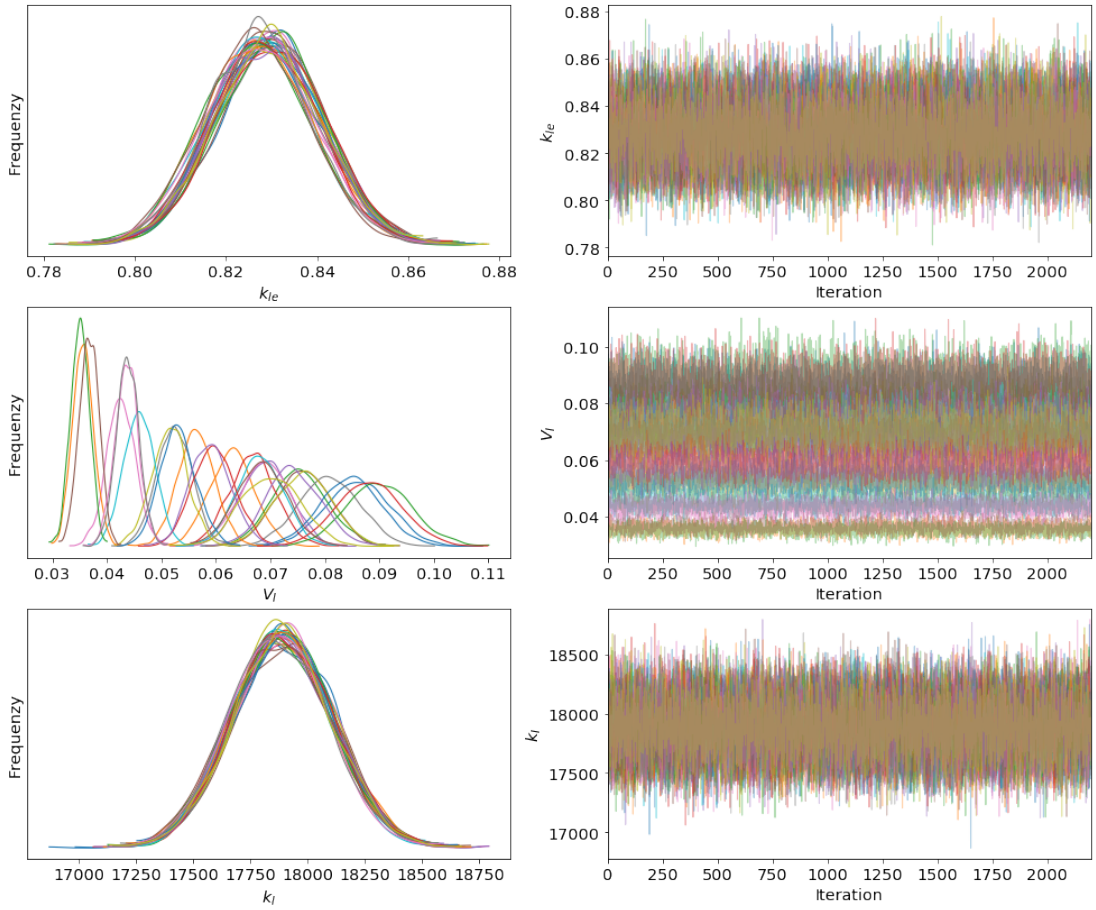

Figure 22: Chains of the Bayesian inference for the parameters. The chains of the three parameter k_{Ie}, V_I and k_I that were estimated are shown from top to bottom. On the right hand side the values the individual chains took during the Bayesian inference are displayed. The left hand side shows smoothed histograms of these values. For clarity reasons only every eighth fit is shown. The fits shown are representative for all fits.

trace plots of k_{eI} and k_I. While the plots of k_{eI} and k_I show a distribution that looks the same for all parameters, the plot of V_I shows a different picture. The traces are located at different values. Looking at the histograms of the traces makes this much evident. In the case of k_{eI} and k_I the individual parameters are located around the same value with distributions that look similar to each other. The histograms in the case of V_I however, are spread out. The distribution differ between higher and lower parameter values. For lower parameter values the distributions are smaller while for higher distributions the distributions are wider. From the trace plot on the right hand side of Fig.22 it can be seen that the density around 0.7 is higher than at the other places. The distribution of k_{eI} and k_I seem to follow a monomodal distribution. Succeeding the discussion of the distributions of the parameters for the insulin fit of the clamp data, monomodal distributions are expected. The spread of the distributions of V_I in this case however can not just justified by arguing with different data sets as the experiments in this data sets are different to each other on purpose and are not supposed to follow the same procedure. A more thorough analysis is therefore necessary.

Seeing that the biggest difference between the experiments should be the insulin infusion rate it is reasonable to look there first. In order to do that the mean parameter values are plotted against the insulin infusion rate used in their experiments. The plots are shown in Fig.23 together with the respective Pearson correlation coefficient. Looking at the plots and the Pearson correlation coefficient the same tendency can be observed in all three parameters. With increasing insulin infusion rates the parameter take lower values. In the case of V_I the changes between the parameter values are of a much bigger

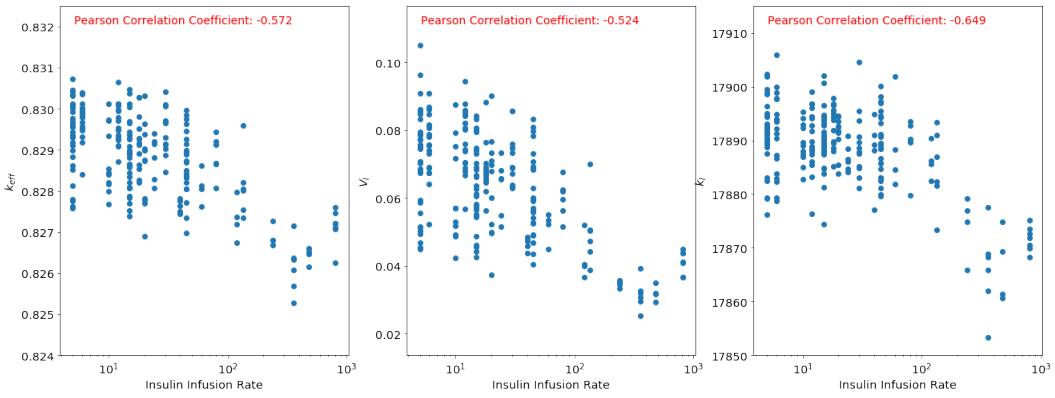

Figure 23: Correlation of the estimated parameters with insulin infusion rate. The estimated parameter values are plotted against the insulin infusion rate used in the respective experiment. The x-axis is in logarithmic scale. All three parameter show correlation. The Pearson correlation coefficient is reported at the top of the figure.

Table 5: Pearson correlation coefficient between the estimated parameters for the insulin fit and the insulin infusion rates and the coefficient of variation for the estimated parameters.

	PCC	CV
k_{eI}	-0.572	0.001
V_I	-0.524	0.25
k_I	-0.649	0.0005

scale than in the case of k_{eI} and k_I. With the coefficient of variation reported in Tab.5 it is clear that the variation of k_{eI} and k_I is very small were as the variation in V_I is quite big. Because of the different scale of changes in the parameters only V_I shows a spread in posterior distributions of the individual experiments in Fig.22. Nonetheless all parameter show a linear correlation between their values and the insulin infusion rate which is supported by the Pearson correlation coefficient as reported in Tab.5. Changing the prior distribution to be more narrow does not yield a different result. The parameters will still show this correlation. The a spread of the prior distribution however is not limited to V_I. With some changes in the priors it is possible to have multimodal distribution similar to the one V_I has in Fig.22 for k_{eI}.

From this it seems as if the fits are fitted by the parameters rather than the dynamics in the model. Even if the fits of the data is not given by the dynamics of the model but by the parameters the validity of the model of interest. For that reason the QQ-plots of the fits in Fig.21 are shown as examples in Fig.24. These plots show that a normal distribution for the model is reasonable assumption. While points are not always following the linear regression exactly they still follow the general trend. A more quantitative analysis is given by looking at the r values of the linear regression. The values lie in the interval [0.63, 1] with a mean of 0.88. This suggest that the model is overall fitted good to the data. While 0.63 is lower than the reported value of the tracer insulin fits it is still high enough to show that model used is valid. The Pearson correlation coefficient between the r values and the insulin infusion rate is given by -0.338. It seems as if the model is valid for both low and the high values with a slight tendency towards a better validity for lower infusion rates.

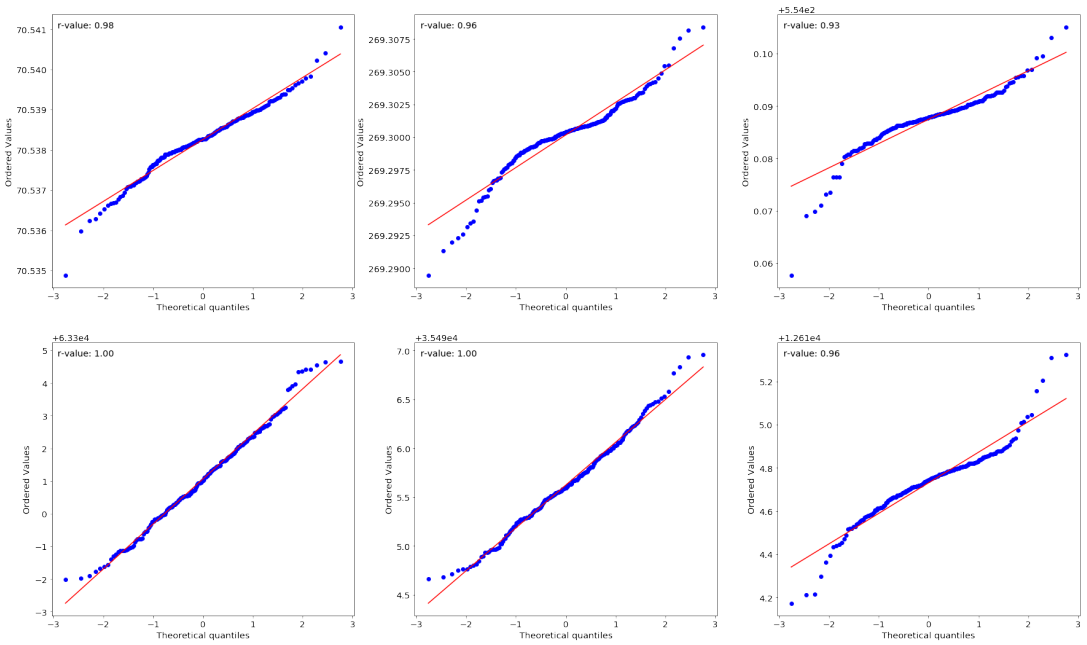

Figure 24: QQ-Plot for insulin fits of the clamp experiments . Six example QQ-plots from the insulin fit are shown with a linear regression fit. The y-axis shows the quantiles of the fits starting at the first measurement point at $t = 60$. The x-axis shows theoretical qunatiles of a normal distribution with mean zero and STD 1. The linear regression is given by the blue line. The respective r-value of the linear regression is displayed in the upper left corner of each plot. In comparison to Fig.20 the linear regression is followed close.

5.4.3 Glucose

The process of determining the parameters for the glucose model in Eq.5.11 is separated into three steps. The first two steps will be performed on the tracer glucose data set while the last one is done with the clamp data set. For all steps the previous determined insulin parameter will be used. In the first step the tracer glucose data will be used. As the dynamics of tracer glucose should be identical to the the dynamics of endogenous glucose any parameter estimated for the tracer model should be able to be used in the glucose model. Using tracer glucose has the benefit of no endogenous glucose production. With no endogenous glucose production, the dynamics of tracer glucose are given by the exogenous input, which is known, and the removal terms. Thereby reducing the parameter that need to be determined. In the second step, the parameter for the endogenous glucose production will be determined using the previous determined glucose removal parameter leaves again fewer parameters to be determined. In the last step, the glucose of the clamp data will be fitted with the parameters of the previous models as

prior.

To determine the parameter of the glucose removal the tracer data is used. As described in Section 4.2 the tracer is initially injected with a bolus at $t = -90$ alongside a constant tracer infusion. At $t = 0$, the constant infusion is replaced by a infusion that is proportional to the injected GIR. As stated in the previous Section 5.3.2 the one compartment model is not able to describe a bolus injection. Starting the fit at $t = -90$ is therefore not possible. Instead it necessary to wait until the bolus is distributed and removed and the dynamics of the tracer glucose is mainly determined by the infusion. The dynamics of the bolus are still in effect at the start of the experiment at $t = 0$. To avoid complications because of that the fit will start at the measurement point at $t = 60$ where the effect of the bolus should have decreased enough for the model to work. Since glucose has an insulin dependence it is necessary to include insulin in the ODE model. With the insulin parameter determined in the previous chapter, they will be fixed. The ODE model used for the fit is then given by,

$$\frac{dI}{dt} = -k_{Ie} I \left(0.8 \frac{k_I V_I}{k_I V_I + I} + 0.2 \right) + X_I, \tag{5.17a}$$

$$\frac{dT}{dt} = -k_{Ge} \frac{T}{k_G V_G + T} \frac{I_{total}}{k_I V_I + I_{total}} + X_T, \tag{5.17b}$$

$$[I] = \frac{I}{V_I}, \tag{5.17c}$$

$$[T] = \frac{T}{V_T}, \tag{5.17d}$$

$$I(60) = I_{exp}(60), \tag{5.17e}$$

$$T(60) = T_{exp}(60). \tag{5.17f}$$

X_I and X_T are the insulin and tracer infusion, respectively. The total insulin concentration follows Eq.5.10. The initial conditions are given by $I_{exp}(60)$ and $T_{exp}(60)$ which are the insulin and tracer measurements at $t = 60$.

The statistical model used for the Bayesian inference in Stan is given by,

$$y_{ij} \sim \mathcal{N}\left(f(t_{ij}; \theta_i), \sigma^2 \right), \tag{5.18a}$$

$$\theta_{ik} \underset{\text{i.i.d.}}{\sim} \text{Lognormal}\left(\log(\beta_k), \omega_k^2 \right), \tag{5.18b}$$

with f being the numerical solution of the model in Eq.5.17 integrated with a fourth and fifth order Runge-Kutta method and $\theta = (k_{Ge}, k_G, V_G)$ being the parameter of the model are going to be fitted.

For the statistical model a normal distribution with a constant error model was used. Since the bolus part of the tracer glucose data is not plotted and the tracer glucose

infusion rate is proportional to the GIR which is is used to keep the glucose at a target value it is reasonable to assume that the tracer glucose will not show huge changes in its concentration. This assumption is supported by the data. A constant error model therefore should be a good fit. The parameters θ follow a log-normal distribution. This allows for the values to be strictly positive defined without having to use a hard constraints to only allow positive parameter values.

Finding values for β_j and ω_j^2 proved to be difficult. Running the Bayesian inference with a broad prior distribution lead to either divergences or saturation of the maximum tree depth. Increasing the tree depth did not lead to better results but increased the running time of the code severely. To increase the chance of convergence better prior distributions needed to be found. In a similar approach as for the insulin, the model was first manually fitted. During this fitting process it became obvious that the parameter θ_j are not independent of each other; they are correlated. It follows that there is more than one possible combination of θ_j's that are capable of fitting the model to the data.

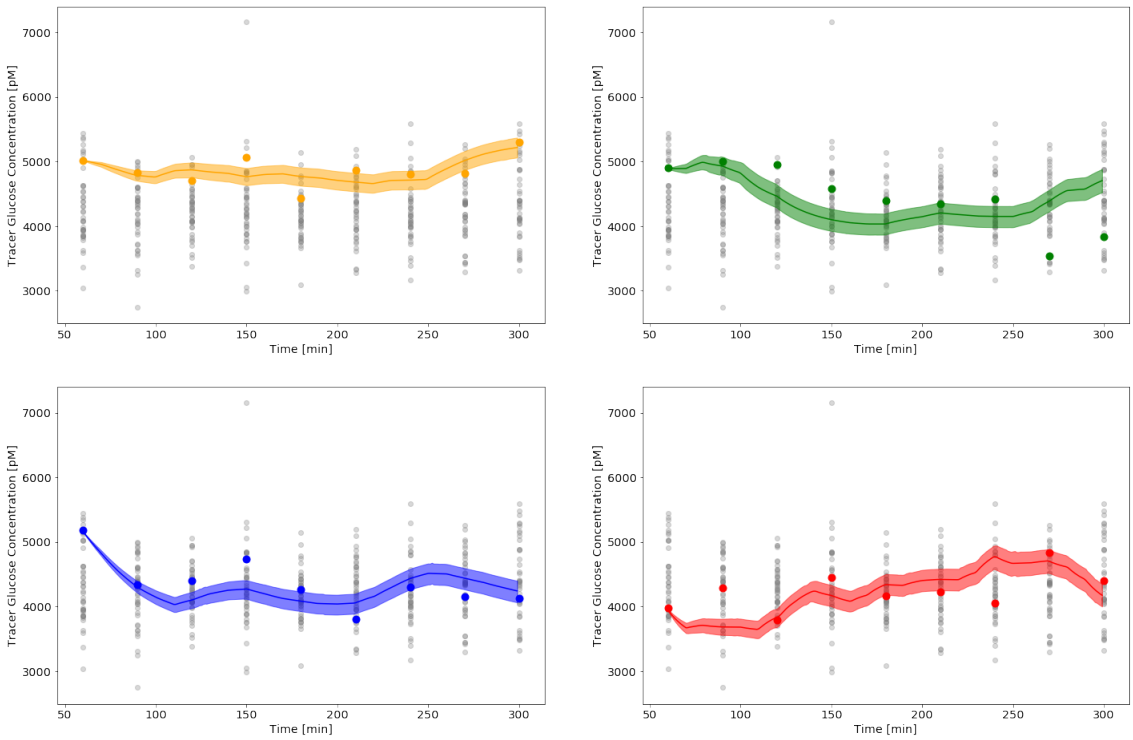

Figure 25: Tracer fits. Four example tracer fits are shown. All tracer measurements are indicated as grey dots. The fitted experiment is shown as bigger colored dots. The fits are given in the same color with their 95% confident interval. The fits are in the same range as the measurements and follow most of the time the general dynamics of the measurement.

With no steady state constraints, the parameter space was only limited to positive values. However, some information about the apparent volume of distribution V_G could be gained from the bolus injection and the following infusion as the are given in amounts while the measurements are in concentrations. With Eq.5.17d a rough estimate of the apparent volume of distribution V_G could be made. That left only the estimation of k_{Ge} and k_G open. The approach to estimate these parameters was to look at k_G first and estimate k_{Ge} accordingly. This approach was chosen as k_G was the Michaelis-Menten constant and as that determines the nonlinear glucose dependent glucose removal. The final values used for β_j and ω_j^2 are reported in Tab.6.
For the Bayesian inference four chains were used with 2000 iterations each of which 1000 iterations were used as a burn-in period. The `adapt_delta` was set at 0.8 and the maximum `tree_depth` was set to 10. In addition to these, thinning was set to 2 to increase the number of effective draws without increasing the memory necessary.
The means and STD of the resulting fit values are in Tab.6. Fig.25 shows four example

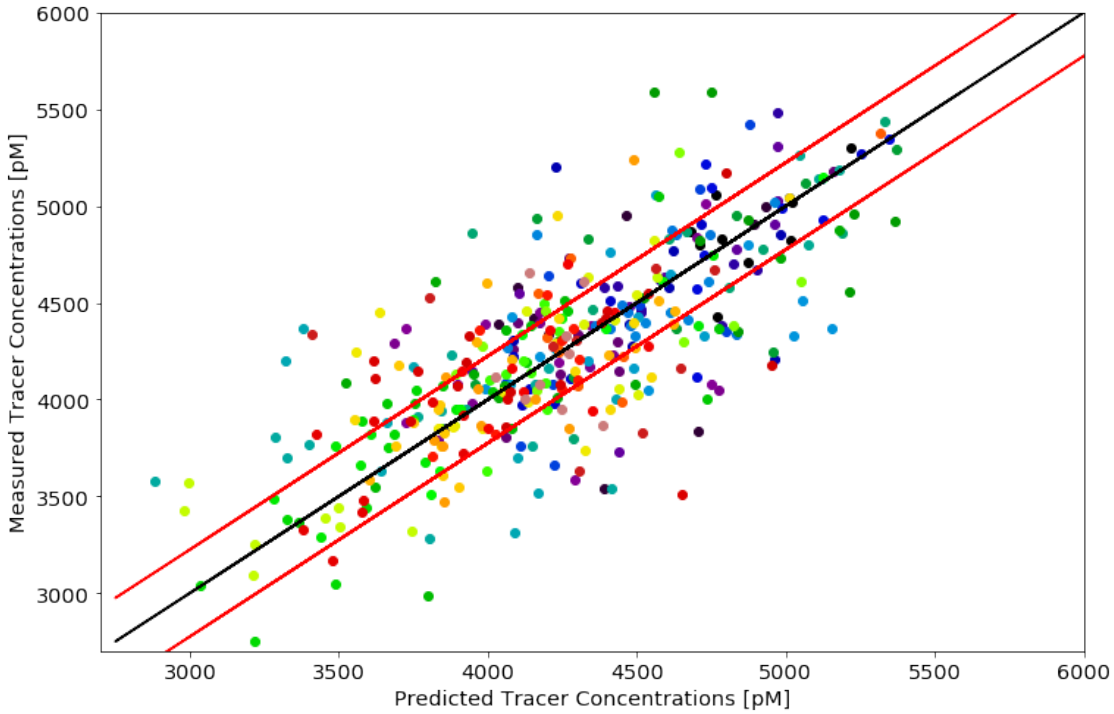

Figure 26: Estimation against observation. The estimated values all experiments are plotted against each other. The black lines indicates the case in which estimation would be equal to the observation with the red line being ±1 STD. From this figure it follows that no systematic errors occur in the fits. Further it can be seen that a significant amount of points lie outside ±1 STD

Table 6: Priors and posteriors for the tracer fits of the tracer data set. Prior values are given before the are log transformed. Posteriors shown are the mean and STD over the mean of all experiments

	Priors		Posteriors	
	Mean	STD	Mean	STD
k_{Ge}	8.5e+03	5e+03	8.11e+03	3.45e+03
V_G	2.6e−01	3e−02	2.59e−01	1.91e−04
k_G	2.45e+04	5e+03	2.41e+04	1.51e+02
σ	2e+02	2e+01	2.24e+02	2.52e−00

fits with their corresponding 95% confidence interval. The fits show an agreement with the data. While the fits are capturing most of the features of data they are not able to describe it entirely. In many cases, the data points even lie outside the 95% confidence interval. However, it does not seem as if the fits have any systematic errors. As there are 44 experiments it is not possible to do a qualitative analysis for all individual fits. For that reason, the predictions of the fits at the time of measurement have been plotted against the observations in Fig.26. The black line shows $y_{fit} = y_{obs}$, with the red lines being ± 1 standard deviation σ, that has been determined during the Bayesian inference, around y_{obs}. Whereas it is difficult to see a single experiment, Fig.26 is able to provide some information about the models ability to fit the data. Fig.26 supports the earlier sentiment that no systematic errors are observed. The data is evenly distributed around the measurements. A distribution of the fitted values that would have been located mainly above or below could have indicated a systematic error in the model. Fig.26 further supports the observation, that the differences between the measurement and the fitted value can be quite large. A significant amount of points lie outside of one standard deviation. While this shows a similar trend as Fig.25 it is notice that the standard deviation in Fig.26 and the 95% confidence intervals in Fig.25 are not the same.

Next the Bayesian inference itself will be evaluated. In Fig.27 the traces of the individual plots for the parameters are displayed. The plots from V_G and k_G show an overlap of the individual histograms from the individual fits. While not being identical but following along the same distribution is what is wanted and what was expected. This behaviour allows for individuality of the the individual while still following a general joint distribution. Looking at the trace plot and the corresponding histogram of k_{Ge} it is, however, quite obvious that this is not the case here. The distributions are spread

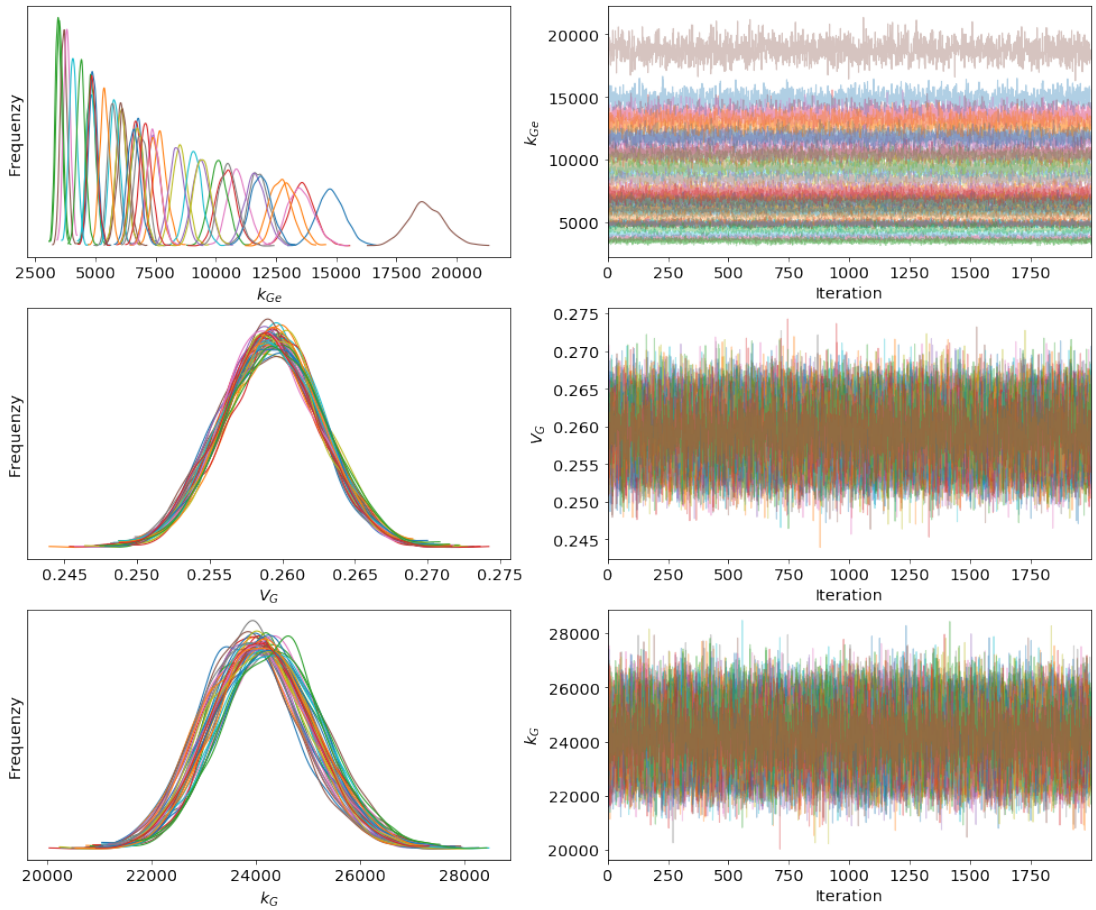

Figure 27: Chains of the Bayesian inference for the parameters. The chains of the three parameter k_{Ge}, V_G and k_G that were estimated are shown from top to bottom. On the right hand side the values the individual chains took during the Bayesian inference are displayed. The left hand side shows smoothed histograms of these values. For clarity reasons only every eighth fit is shown. The fits shown are representative for all fits. The distributions of the estimated parameters for the individual experiment of V_G and k_G lie close to each other. The distributions of k_{Ge} however are spread out.

out over a range of almost one magnitude and are mostly not aligned with each other. They all follow a monomodal distribution but without seeming to have a general joint distribution. Combining the histograms together yields a multimodal distribution that does not agree with our prior distribution of a log-normal. As mentioned above, during the manual fitting of the model a correlation between the parameters was observed. From the trace plots and histograms no correlation can be observed. looking at the pair plot in Fig.28 shows that the parameters are not uncorrelated. Indeed, k_G and k_{Ge} are correlated while V_G is independent of either of them. Because of the multimodal

distribution of k_{Ge} any pair plot with it will display these modes. These plots can still show a correlation between parameters as in the independent case all modes should be evenly distributed as can be see in the pair plot of k_{Ge} and V_G. The plot between k_{Ge} and k_G on the other hand show that the values are not independent of each other. This observed correlation between k_G and k_{Ge} during the manual fitting is confirmed by Fig.28. It is not surprising that any variation of the model manifests in k_{Ge} as both, k_G and V_G, have pretty strict priors whereas the prior for k_{Ge} was left loose. With a more strict prior it was not possible for the Bayesian inference to fit all the parameters. The cause for the variation in k_{Ge} can be tracked to the insulin infusion rates. Plotting the k_{Ge} values in dependence of the insulin infusion rate shows a clear correlation between the two. Indeed, the plot looks pretty similar to the resulting plot of the mean tracer infusion rate versus the insulin infusion rate. From here it follows that the insulin dependent glucose removal is not working as intended.
To validate the statistical model of the fit, Eq.5.18, Q-Q plots are used. Fig.29 shows six

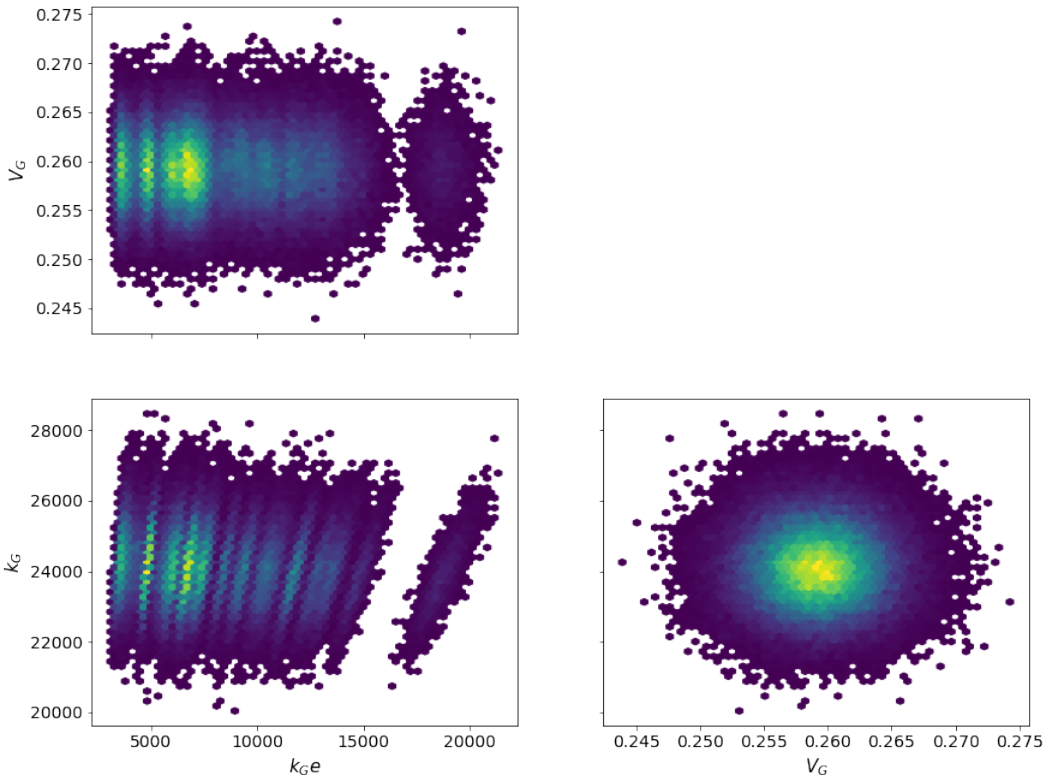

Figure 28: Pair plot of estimated values of the parameters. The estimated values of all three parameters of all experiments are plotted against each other. From the plots it can be seen, that V_G shows no correlation with any other parameter. Between k_{Ge} and k_G a correlation is visible.

example plots. Q-Q plots are used to verify if our model is follows a normal distribution as hypothesized in the statistical. Looking at the plots, the quantiles follow the fitted linear regression in a wave like pattern. This indicates that the values produced by the Bayesian inference follows a normal distribution. However, the wave like pattern would suggest that the posterior distribution has heavier tails or is more skewed. The S shape in these seem to be more pronounced than in the Q-Q plots of the insulin fits.
With the fit of the tracer data done and validated the next step of the parameter estimation of the glucose model can be looked at. As lined out in the beginning of the chapter the next step is to determine the parameter of the EGP. To do so, the tracer-glucose relation will be used. As the the tracer should follow the same dynamics as the glucose, the previously determined parameter k_{Ge}, V_G and k_G will be used as fixed parameters for the glucose model. Since the tracer data and the glucose data were measured in the same experiment, fixing the parameters should yield a working glucose

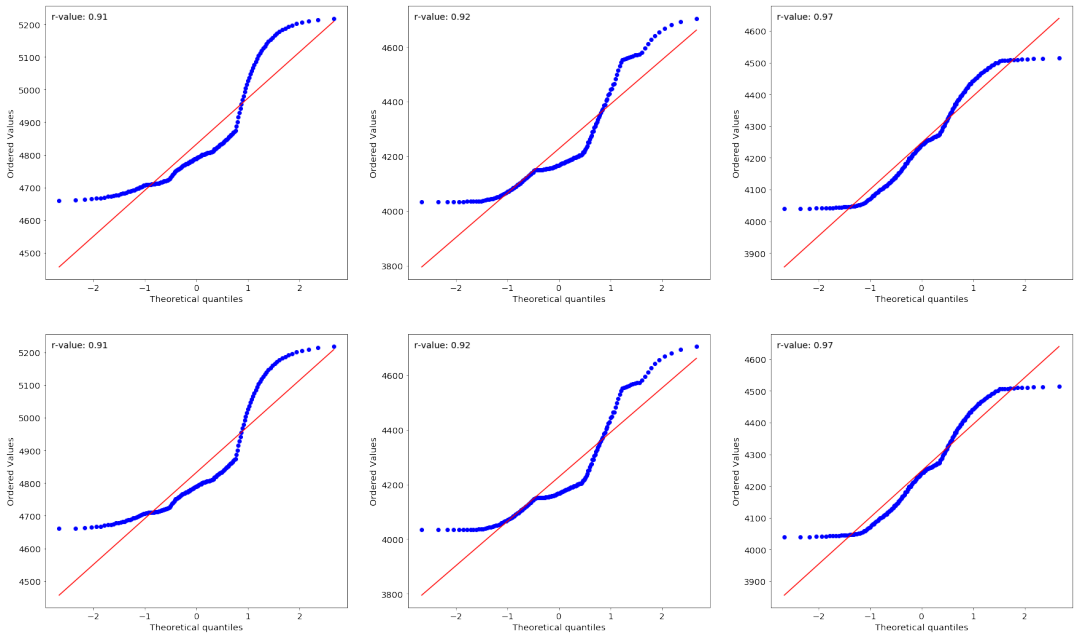

Figure 29: QQ-Plot for glucose tracer fits. Six example QQ-plots from the insulin fit are shown with a linear regression fit. The y-axis shows the quantiles of the fits starting at the first measurement point at $t = 60$. The x-axis shows theoretical qunatiles of a normal distribution with mean zero and STD 1. The linear regression is given by the blue line. The respective r-value of the linear regression is displayed in the upper left corner of each plot. The plots show a stronger S shape than both QQ-plots of insulin plots. This indicates that the distribution of the tracer fits is more skewed or has heavier tails then the distributions of the insulin fits.

removal in the glucose model. The EGP will then be fitted using Bayesian inference again.

The model that will be fitted is given by,

$$\frac{dI}{dt} = -k_{Ie} I \left(0.8 \frac{k_I V_I}{k_I V_I + I} + 0.2 \right) + X_I, \tag{5.19a}$$

$$\frac{dG}{dt} = EGP - k_{Ge} \frac{G}{k_G V_G + G} \frac{I_{total}}{k_I V_I + I_{total}} + X_G, \tag{5.19b}$$

$$EGP = \max(k_{EGP,0} - k_{EGP,G} G - k_{EGP,I} I, 0), \tag{5.19c}$$

$$[I] = \frac{I}{V_I}, \tag{5.19d}$$

$$[G] = \frac{G}{V_G}, \tag{5.19e}$$

$$I(-30) = 0, \tag{5.19f}$$

$$T(-30) = T_{exp}(-30). \tag{5.19g}$$

with the parameters being defined as above and X_I and X_G being the insulin and GIR, respectively.

The statistical model follows Eq.5.18 with f being the numerical solution of Eq.5.19b and $\theta = (k_{EGP,0}, k_{EGP,G}, k_{EGP,I})$. β_j and ω_j^2 are the corresponding values defining the prior distribution.

For the fitting of the EGP a similar approach as in the fits before have been used. An initial run of the model was done with the only prior being that all parameters need to be positive. The fit did not converge. For a higher chance of convergence, better priors are needed. Again following the approach from the fits before, the EGP was fitted manually. During that process two problems arose.

First, the parameters of the EGP are correlated. Looking at Eq.5.19c the dependence is quite obvious. However, a limitation is given by $k_{EGP,0}$ as $k_{EGP,0}$ needs to be at least be big enough to provide a steady state when $k_{EGP,G} = k_{EGP,I} = 0$. This still leaves a huge range for all three parameters.

Second, the glucose measurements can be separated into two phases, $t < 0$ before the experiment and $t \geq 0$ the experiment. For $t < 0$, the system should be in a steady state. Neither the GIR nor the insulin infusion have started at that time. The EGP should produce glucose. For $t \geq 0$, the steady state system is perturbed. GIR and insulin infusion have started. During that phase the EGP could be active all the time, active some times or inactive all the time depending on the glucose and insulin blood concentrations. Over the two phases, the glucose blood concentration changes only slightly while the insulin blood concentration increases significantly. The difficulty is find pa-

rameters that are able to describe both phases at the same time. To get a better feel for the problem the EGP can be simplified. Since the blood glucose concentration is not changing a lot, $k_{EGP,G} \cdot G$ can be assumed constant. With $k_{EGP,G} \cdot G$ assumed constant the EGP can be reduced to two parameters given by $EGP = k_{EGP,0G} - k_{EGP,I} I$ with $k_{EGP,0G} = k_{EGP,0} - k_{EGP,G} G$.

Even with this simplification, it was not possible to fit Eqs.5.19b. The EGP could be adjusted to fit the steady state phase or the experimental phase but not both at the same time. Fig. shows an example fit of the solution of the model described in Eqs.5.19b for three cases: $EGP = 0$, EGP fitted for the steady state phase and EGP fitted for the experimental phase. The fitting has been performed by hand and is mainly illustrative. In the case of $EGP = 0$ (green line), the glucose concentration is decreasing until

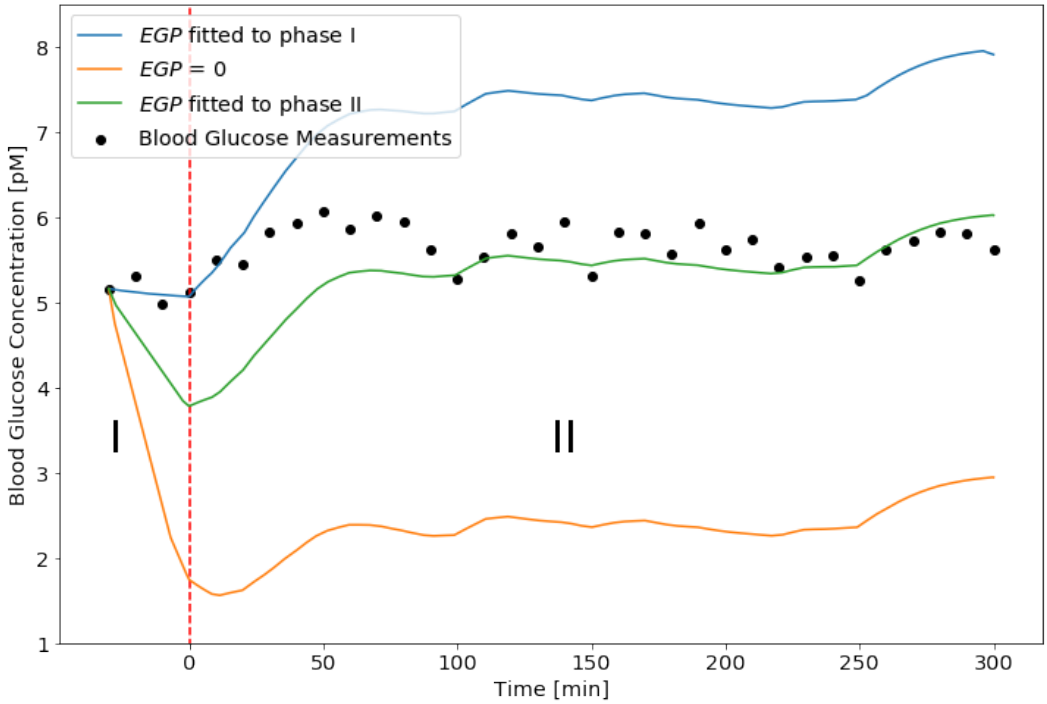

Figure 30: Plot of glucose for different configurations of the EGP. Three different configuration of the EGP are plotted. The data is separated into two phase, $t < 0$ and $t \geq 0$. The other parameter values are were taken from previous fits of the tracer glucose and insulin. The orange line shows the plot of the glucose model with no EGP. No phase is described good. The blue line shows a plot where the EGP is fitted for first phase. The second phase is described in a good way. For the green line the EGP was fitted to the second phase. Only after an initial stabilisation the second phase is described well. The first phase is not described good.

$t = 0$ when the GIR sets in and the blood glucose concentration stabilizes between 2 and 3 pM. The curve follows the dynamics of the glucose measurements but with an offset. When fitting for the steady state phase (blue line), the first few data points are fitted well but at $t = 0$ the blood glucose concentration raises until it stabilizes between 8 and 7 pM, above the measurement. Again, the dynamics of the measurement are followed but with an offset. In the last case, when the EGP is fitted for the experimental phase (green line), the blood glucose concentration in the steady state phase is decreasing until $t = 0$ where it it starts to raise until it stabilizes around the measurement points. The dynamics of the measurements are followed again.

All three fits are able to follow the dynamics of the model with or without an offset at different times. However, non was able to describe the blood glucose concentration for the whole duration of the measurement. Without being able to describe the EGP and therefore not being able to fit the blood glucose dynamics, no further analysis of the model has been done. While it would have been possible to fit the data in a similar way as the tracer glucose, by removing the part that can not be described by the model, it would have been a bigger limitation to the models capabilities.

The reason why it is not possible to estimate the EGP and therefore the fit the glucose is difficult to determine. One possibility would be, that the chosen EGP term is not capable of capturing the dynamics. At the moment that would be difficult to show. Another possibility would be, that the glucose model has shortcomings in its description of the glucose removal. With the tracer model being able to capture the tracer dynamics and the plots of the glucose in Fig.30 also being able to capture the dynamics even though they are offset it seems unlikely that the problematic lies within the glucose dependent glucose removal. However, the problem might lie within the insulin dependent glucose removal. As can be seen from Fig.30 blue plot, when the EGP is fitted to capture the steady state the model gives too high of glucose output over the whole duration of the experiment. As the insulin is in a steady state for most of the experiment, see e.g. Fig.21, it might be possible that insulin dependent removal of glucose is underestimated. Possible complications with the insulin dependent glucose removal could be due to the simplification made in the model, where the Michaelis-Menten constant from the insulin model was also used for the glucose model. This underestimation of the insulin removal could also be the reason why the parameter values of k_{Ge} were correlated to the the insulin infusion rate and therefore to the insulin steady state values.

6 Conclusion

In this thesis two models for the euglycemic hyperinsulinemic clamp experiment were proposed and examined by fitting to experimental euglycemic hyperinsulinemic clamp experiment data from rats using Bayesian inference in Stan. To fit the individual data, a hierarchical model has been used. The distributions of the individual parameters were expected to follow a the same population distribution with some variation between the parameters.

The first model proposed was a model of the insulin glucose system consisting of two two-compartment models for insulin and glucose each that interact with each other. Similar models have been proposed before, e.g. [18]. However, the data sets used show a behaviour that offers a different approach to some of the terms in the model. The new proposed terms should allow for the model to describe the euglycemic hyperinsulinemic clamp experiment for low and very high insulin infusion rates. In the initial step it was attempted to fit the model to IV data. It proved, however, to be not possible to fit the proposed hierarchical model to the data. While a simplified version of the model was able to describe the data, as can be seen in Fig.32, it was not possible to fit it in a hierarchical fashion for all parameters. It was considered if even the simplified version of the model was too complex for to be fitted. However, it is known that the simplified version of the model is *apriori* identifiable and therefore should be able to be fitted. Other reasons that were considered are the quality of the data and the Bayesian inference used. Without being able to determine the reason for the inability to fit the model it was decided that moving forward a less complex version of the model will be used.

The reduced model only contained a one-compartment model for both insulin and glucose. With the reduction of the model, it follows that some dynamics of the glucose insulin system can not be described anymore, mainly IV curves. This, however, should not hinder the models ability to describe the euglycemic hyperinsulinemic clamp experiment. In the first step the model was used to describe the insulin measurements of the experiments. As can be seen in Fig.21a and 21b the model was able to capture the these. But, further analysis showed that a correlation between the parameters and the infusion rate exists. This finding suggest that it was not the terms of the model that captured the changing dynamics but the parameters. In the next step the model was used to describe the glucose dynamics. For that tracer measurements were analysed. Fig.25 shows that the model was able to capture the dynamics of the model. But, similar to the insulin fit, the fit was driven by the parameters and not the dynamics of the terms. In the last step, the glucose was to be fitted by using the previously determined parameters from the tracer fit to find the values of the EGP. This proved not to be

possible. Possible reason for that are that are a wrong implementation of the EGP or even errors in the model that lead to the point that the EGP could not be estimated. In conclusion, the proposed models did not work. While the reduced model was able to capture some of the dynamics, it was not due to dynamics implemented in the model but due to the parameter changing.

6.1 Outlook

As the proposed model was not able to describe the observations from the euglycemic hyperinsulinemic clamp experiments a new approach needs to be found. A first starting point could be to look at the simplifications made in this model and see if they were the reason for the failure. If this yields no results, a new approach for the removal of insulin is needed.

Another possibility would be to try out a different approach to the estimation of the parameters of the model. It is possible that the inability of the fitting of the model does not lie within the model but within the approach and the program used. In this thesis no cross validation between different fitting methods were used nor were different platforms for Bayesian inference considered.

References

[1] P. Palumbo, S. Ditlevsen, A. Bertuzzi, and A. De Gaetano, "Mathematical modeling of the glucose–insulin system: A review," *Mathematical biosciences*, vol. 244, no. 2, pp. 69–81, 2013.

[2] H. J. Woerle and J. E. Gerich, "Glucose physiology, normal," in *Encyclopedia of Endocrine Diseases* (L. Martini, ed.), pp. 263–270, New York: Elsevier, 2004.

[3] C. Anderwald, A. Tura, A. Grassi, and et al, "Insulin infusion during normoglycemia modulates insulin secretion according to whole-body insulin sensitivity," *Diabetes Care*, vol. 34, no. 2, pp. 437–41, 2011.

[4] W. C. Duckworth, R. G. Bennett, and F. G. Hamel, "Insulin degradation: progress and potential," *Endocrine reviews*, vol. 19, no. 5, pp. 608–624, 1998.

[5] G. Wilcox, "Insulin and insulin resistance," *Clinical biochemist reviews*, vol. 26, no. 2, p. 19, 2005.

[6] C. Anderwald, A. Tura, A. Grassi, M. Krebs, J. Szendroedi, M. Roden, M. G. Bischof, A. Luger, and G. Pacini, "Insulin infusion during normoglycemia modulates insulin secretion according to whole-body insulin sensitivity," *Diabetes Care*, vol. 34, no. 2, pp. 437–441, 2011.

[7] M. Kohlmeier, "Glucose," in *Nutrient Metabolism* (M. Kohlmeier, ed.), Food Science and Technology, pp. 193–210, London: Academic Press, 2003.

[8] S. L. Aronoff, K. Berkowitz, B. Shreiner, and L. Want, "Glucose metabolism and regulation: Beyond insulin and glucagon," *Diabetes Spectrum*, vol. 17, no. 3, pp. 183–190, 2004.

[9] G. M. Kowalski and C. R. Bruce, "The regulation of glucose metabolism: implications and considerations for the assessment of glucose homeostasis in rodents," *American Journal of Physiology-Endocrinology and Metabolism*, vol. 307, no. 10, pp. E859–E871, 2014.

[10] B. M. Mouri MI, "Hyperglygemia. [updated 2020 sep 10]," in *StatPearls [Internet]*, Treasure Island (FL): StatPearls Publishing, 2021 Jan.

[11] S. Kalra, J. Mukherjee, S. Venkataraman, and et al., "Hypoglycemia: The neglected complication," *Indian J Endocrinol Metab.*, vol. 17, 2013.

[12] M. Lavielle, *Mixed Effects Models for the Population Approach: Models, Tasks, Methods and Tools*. Chapman and Hall/CRC, 2014.

[13] A. Gelman, J. B. Carlin, H. S. Stern, D. B. Dunson, A. Vehtari, and D. B. Rubin, *Bayesian data analysis*. CRC press, 2013.

[14] L. Shargel and A. Yu, *Applied Biopharmaceutics & Pharmacokinetics, Seventh Edition*. McGraw-Hill Education, 7th ed., 2016.

[15] G. T. a. Claudio Cobelli, David Foster, *Tracer Kinetics in Biomedical Research: From Data to Model*. Springer US, 1 ed., 2002.

[16] M. P. Saccomani, L. D'Angio, S. Audoly, C. Cobelli, L. D'Angio', and S. Audoly, "Chapter 4 - a prioriidentifiability of physiological parametric models," in *Modeling Methodology for Physiology and Medicine* (E. Carson and C. Cobelli, eds.), Biomedical Engineering, pp. 77–105, San Diego: Academic Press, 2001.

[17] K. R. Godfrey and M. J. Chapman, "The problem of model indistinguishability in pharmacokinetics," *Journal of pharmacokinetics and biopharmaceutics*, vol. 17, no. 2, pp. 229–267, 1989.

[18] C. Dalla Man, R. A. Rizza, and C. Cobelli, "Meal simulation model of the glucose-insulin system," *IEEE Transactions on biomedical engineering*, vol. 54, no. 10, pp. 1740–1749, 2007.

[19] R. N. Bergman, Y. Z. Ider, C. R. Bowden, and C. Cobelli, "Quantitative estimation of insulin sensitivity.," *American Journal of Physiology-Endocrinology And Metabolism*, vol. 236, no. 6, p. E667, 1979.

[20] R. Hovorka, F. Shojaee-Moradie, P. V. Carroll, L. J. Chassin, I. J. Gowrie, N. C. Jackson, R. S. Tudor, A. M. Umpleby, and R. H. Jones, "Partitioning glucose distribution/transport, disposal, and endogenous production during ivgtt," *American Journal of Physiology-Endocrinology and Metabolism*, vol. 282, no. 5, pp. E992–E1007, 2002.

[21] C. D. Man, G. Toffolo, R. Basu, R. A. Rizza, and C. Cobelli, "A model of glucose production during a meal," in *2006 International Conference of the IEEE Engineering in Medicine and Biology Society*, pp. 5647–5650, 2006.

[22] U. Picchini, A. De Gaetano, S. Panunzi, S. Ditlevsen, and G. Mingrone, "A mathematical model of the euglycemic hyperinsulinemic clamp," *Theoretical Biology and Medical Modelling*, vol. 2, no. 1, pp. 1–11, 2005.

[23] U. Picchini, S. Ditlevsen, and A. De Gaetano, "Modeling the euglycemic hyperinsulinemic clamp by stochastic differential equations," *Journal of mathematical biology*, vol. 53, no. 5, pp. 771–796, 2006.

[24] K. R. Godfrey, M. J. Chapman, and S. Vajda, "Identifiability and indistinguishability of nonlinear pharmacokinetic models," *Journal of pharmacokinetics and biopharmaceutics*, vol. 22, no. 3, pp. 229–251, 1994.

[25] B. Carpenter, A. Gelman, M. D. Hoffman, D. Lee, B. Goodrich, M. Betancourt, M. Brubaker, J. Guo, P. Li, and A. Riddell, "Stan: A probabilistic programming language," *Journal of statistical software*, vol. 76, no. 1, 2017.

[26] M. D. Hoffman and A. Gelman, "The no-u-turn sampler: Adaptively setting path lengths in hamiltonian monte carlo," *Journal of Machine Learning Research*, vol. 15, no. 47, pp. 1593–1623, 2014.

A Tracer Models

A.1 Two-Compartment Model

The model for the tracer glucose follows Eqs.5.4 pretty close. With tracer glucose not being able to be produced by the body, no EGP term is necessary. Further the insulin independent clearance of glucose, F_{CNS}, needs to be scaled as $G \gg T$. For that simply the fraction of the two amounts is taken.
The model is then given by,

$$\frac{dT_C}{dt} = -k_1 T_C + k_2 T_P - \frac{T_C}{G_C} F_{CNS}, \tag{A.1a}$$

$$\frac{dT_P}{dt} = k_1 T_C - k_2 T_P - n_{GP} G_P \frac{T_P}{k_{GP} V_{GP} + T_P} \frac{I_{P,total}}{k_{IP} V_{IP} + I_{P,total}}, \tag{A.1b}$$

$$[T_j] = \frac{T_j}{V_{Gj}}, \text{ for} j = C, P, \tag{A.1c}$$

with T_C, T_P, $[T_P]$ and $[T_C]$ being the glucose amounts and concentrations in the central and peripheral compartment. k_1 and k_2 are the transfer rates between the central and the peripheral compartment, V_{GC} and V_{GP} are the apparent volume of distribution of the central and peripheral compartment, F_{CNS} is the insulin independent glucose uptake of the central nervous system, n_{GP} is the removal rate parameter in the peripheral compartment, k_{GP} and k_{IP} are Michaelis-Menten constants for a glucose dependence and a insulin dependence in the peripheral compartment, respectively and $I_{P,total}$ is the total insulin concentration in the peripheral compartment.

A.2 Reduced Model

The tracer model follows the glucose model Eq.5.11 very close again. Like in the previous model the EGP term is removed and all the other terms are kept. The tracer model is therefore given by,

$$\frac{dT}{dt} = -k_{Ge} \frac{T}{k_G V_G + T} \frac{I_{total}}{k_I V_I + I_{total}} \tag{A.2a}$$

$$[T] = \frac{T}{V_G}, \tag{A.2b}$$

with T, $[T]$ being the glucose tracer amount in the blood and blood glucose tracer concentration, respectively and the other parameters being the same as described in the glucose model.

B Parameter Estimation Two-Compartment Model

The model that is to fit the data is given by Eqs.5.1, 5.2, 5.3, 5.4, 5.6, 5.7 and A.1. It contains a total of 15 parameters.
The size of the model does not allow for to fit everything in go. The plan was to determine all the parameter in an iterative fashion. The parameters determined in previous iterations will then be used to determine the remaining parameters building up. In the first step steady state conditions and extrapolation are used to reduce the parameter need to be estimated by fitting as much as possible. This step has been done in Section 5.4.1. The next step is to use the IV data for the insulin concentrations and the tracer concentrations. These should be able to yield the transfer rates in both models. The next step would be to use only the insulin data to determine the parameters in the removal term. In the next step the tracer data will be fitted. The tracer fit has the benefit of not having a EGP and therefore reducing the amount of parameters needed to be determined in one fit. In the next and final step the clamp data will be fitted. Using all the information gained in the previous fits only the EGP needs to be determined without any prior knowledge.

B.1 IV Fits

The goal in this section is to use the IV data to determine as many parameters as possible. The priority however lies on determining the transfer rates k_{12}, k_{21} and k_1, k_2 for the insulin and the glucose model, respectively.
For the fitting a statistical model needs to be set up. As the goal is to describe and capture the variance between the individual rats a hierarchical model will be used. The insulin and glucose fit will use the same structure for their statistical model. The structure of the model is given by,

$$y_{ij} \sim \mathcal{N}\left(f(t_{ij};\theta_i), f(t_{ij};\theta_i)\sigma^2\right) \tag{B.1a}$$

$$\theta_{ij} \underset{\text{i.i.d.}}{\sim} \mathcal{N}\left(\log(\beta_j), \omega_j^2\right), \tag{B.1b}$$

following the general definition of hierarchical models in Eq.3.7.
For the function $f(t_{ij}, \theta_i)$ the numerical solution of Eq.5.1 and Eq.A.1 will be used for the insulin and the tracer fit, respectively. As the IV data spans over multiple orders of magnitude a proportional error model is used. The θ_i are the fit parameters from the models. Since all parameters in the model are defined as larger then zero a log-normal prior is used in Eq.B.1b.
For the IV fit of the tracer model some assumptions are necessary. Since no insulin data

is provided in the tracer IV data set we assume basal insulin levels. Additionally we assume that the infusion of tracer glucose does not disturb the system as in all tracer experiment. The insulin levels are therefore taken as constant.
The initial conditions for the tracer IV fit are given by

$$T_C(0) = T_{bolus} \tag{B.2a}$$

$$T_P(0) = 0. \tag{B.2b}$$

Since tracer glucose is not produced endogenously and is not injected prior to the start of the experiment its amount in the central compartment is equal to bolus amount while the amount in the peripheral compartment is zero.
This left seven parameters to be determined in the fit. Running Bayesian inference on this model yielded no results. Determining the seven parameters without prior knowledge of their values proved not to be possible. As the main interest of the IV data were the transfer rates the model was simplified.
In order to reduce the amount of parameters the removal term in the peripheral compartment got reduced to a linear removal term depending on the tracer concentration in the peripheral compartment. The resulting model takes the form,

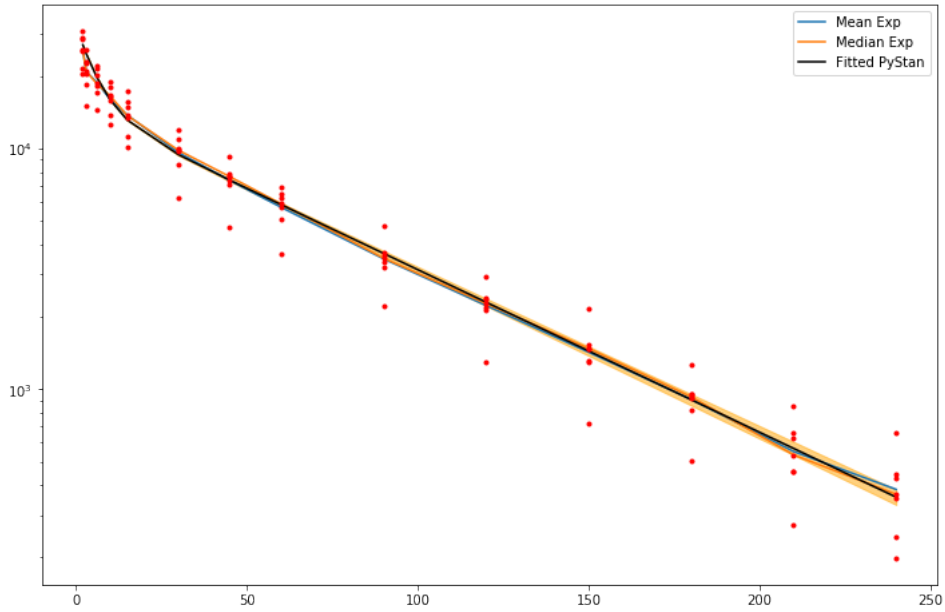

Figure 31: Mean fit of the tracer glucose IV curves. All tracer IV curves are fitted at the same time for one set of parameter. In this setup it was possible to fit the whole model.

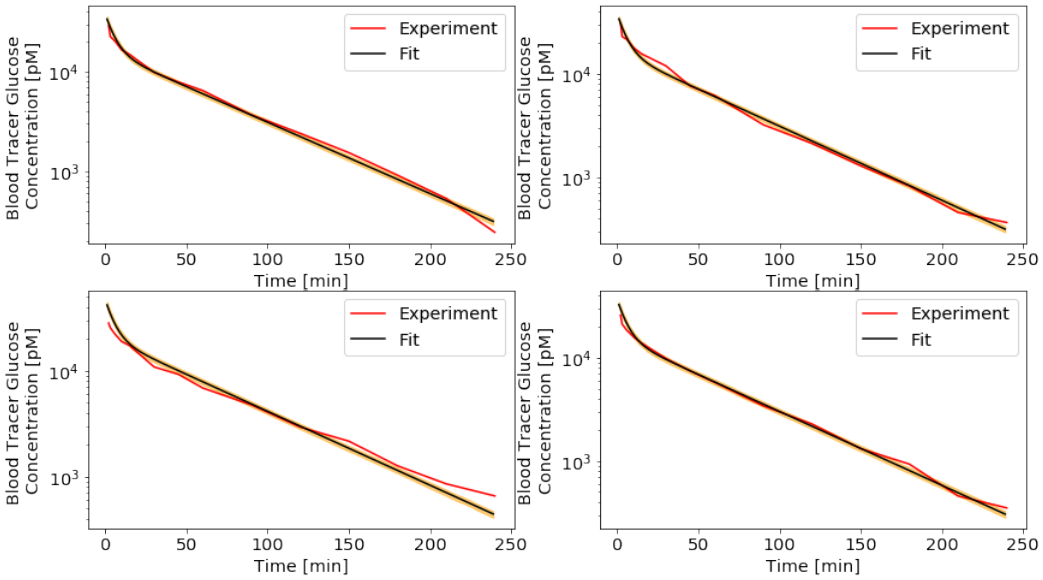

Figure 32: Tracer fit of the IV curves. Four example fits of the glucose tracer IV curves are shown. The dynamics of the curve are well described. However, it was not possible to fit the whole model to curves. The removal rate has been fixed in this case.

$$\frac{dT_C}{dt} = -k_1 T_C + k_2 T_P \tag{B.3a}$$

$$\frac{dT_P}{dt} = k_1 T_C - k_2 T_P - V_{TP} T_P, \tag{B.3b}$$

reducing the number of parameters needed to be determined from seven to four. The initial conditions are unchanged.

Using Eq.B.3 the fits in Fig.31 are produced.

The initial conditions for the insulin fit are similar to the tracer ones. As the injected insulin is a different analogue then the endogenous insulin the blood insulin will be zero prior to the injection. Thus at the time of injection the insulin concentration in the two compartments is given by

$$I_C(0) = I_{bolus} \tag{B.4a}$$

$$I_P(0) = 0. \tag{B.4b}$$

For the insulin fit we followed the approach from the tracer IV fits and simplified the model. Opposed to the tracer model the insulin model contains a removal term in both compartments. The simplification can therefore be done in multiple ways.

The four simplification considered here all follow a similar structure; the removal terms

in each compartment are either linearized or removed. The model will take the form

$$\frac{dI_C}{dt} = k_{21}I_P - k_{12}I_C - V_{IC}I_C \tag{B.5a}$$

$$\frac{dI_P}{dt} = -k_{21}I_P + k_{12}I_C - V_{IP}I_P \tag{B.5b}$$

with 1.) $V_{IC} \neq 0$ and $V_{IP} \neq 0$, 2.) $V_{IC} = V_{IP} \neq 0$, 3.) $V_{IC} = 0$ and $V_{IP} \neq 0$, and 4.) $V_{IC} \neq 0$ and $V_{IP} = 0$ for the four simplifications considered.
1.) is closest to the full model as it has a removal rate in each compartment with different removal rates between them. It therefore has the largest number of parameters that needs to be determined. Simplification 2.) also has a removal term in each compartment but the removal rates are set to be the same. Reducing the number of parameters that need to be determined by one. The simplifications 3.) and 4.) both have one removal term, in the central and in peripheral compartment, respectively. They have the same amount of parameters as 2.) but the dynamics are more simple.

B.2 Results and Discussion

The fits of the IV data for insulin and tracer proved difficult as it was not possible to do the hierarchical fits describe in SectionB.1. It was, however, possible to use all data points to estimate one set of parameters for both the insulin and tracer IV data. The fit for the tracer IV is displayed in Fig.31
While Fig.31 shows that the simplified tracer model is able to describe the dynamics seen in the tracer IV curves Stan was unable to fit the hierarchical model. Even more surprisingly Stan was not able to fit individual curves consistently even when presented with very good priors, e.g. parameter values from the average fit. Fixing one parameter and thereby reducing the number of parameters needed to be estimated yielded in a positive change. With only three parameters to be estimated individual IV curves could be fitted reliably. Furthermore it was possible to run the hierarchical model. The fit of each individual curve is shown in Fig.32. As we are mostly interested in the transfer rates k_1, k_2 the removal rate V_M was set constant to the value determined in fit of the average.
Similar to tracer IV fit the insulin IV curves could be described by model, however it proved not to be possible to fit a hierarchical model to the IV data provided in the data set. Applying simplification to the model to reduce the number of parameters that need to be determined did not suffice in making the fit of the hierarchical model possible. It was however possible to fit the average of the model using all the data provided. This, at least, shows that the model is capable of capturing the dynamics to some extent.

Using the parameter estimated this way as prior while fixing one of them allowed for the fitting of the hierarchical models. It follows from here that the single IV curves do not provide enough data to allow the estimation of all the parameters of the model for the fitting with Bayesian inference.
An indicator to whether to problem lies within the model to fit, the data or the fitting algorithm could be gotten by an *a priori* analysis of the models. In fact, for the simplified models used for the IV fits in the end *a priori* analysis have been performed [24]. The simplified tracer model as well as the simplifications 3.) and 4.) for the insulin model are identifiable, simplification 1.) is unidentifiable and simplification 2.) is not mentioned. As the simplification 1.) of the insulin model is the only one that could not be fitted at all it seems like that the models are conform with the *a priori* analysis. This, however, does not provide any additional information on why the hierarchical model failed while the average model worked.
As we are unable to use hierarchical models for the simplest model we decided to use a different model and keep working with Bayesian inference and Stan.

C Markov Chain Monte Carlo and No-U-Turn Sampler

To use Bayesian inference for parameter estimation programs have been developed. The program used in this thesis for Bayesian inference is Stan [25]. Stan is platform for statistical modeling and high-performance statistical computational.
Bayesian statistical inference in Stan is implemented through two Markov Chain Monte Carlo (MCMC) algorithms, the Hamiltonian Monte Carlo (HMC) algorithm and its adaptive variant the no-U-turn sampler (NUTS). MCMC is a method for constructing and sampling from an posterior distribution. The method is based on drawing values of θ from an approximate distribution and then correcting these to better approximate the target distribution $p(\theta|y)$. The approximate distribution therefore should converge towards the target distribution with every step in the simulation. The distribution of the sampled draws depends only on the last drawn value and therefore forms a Markov Chain.
Fig.33 shows a simple example of a Markov Chain simulation using a Metropolis algorithm with two parameters θ that both follow a normal posterior distribution $N \sim \mathcal{N}(0, I)$. While the Bayesian inference shown in Fig.33 uses a Metropolis algorithm the general idea is the same as in the algorithm used in Stan. In the figure five chains with different initial positions are shown. The black dots indicate their initial position. From

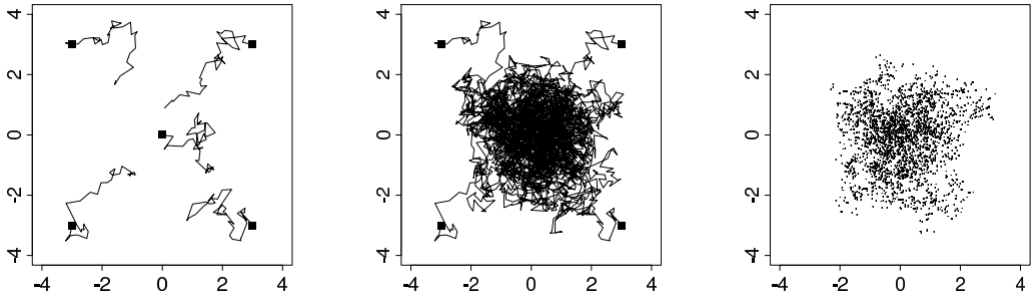

Figure 33: Markov Chain simulation. Five independent sequences of a Markov Chain simulation with two parameters both following a normal distribution. Starting points are indicated by black squares. The lines from each square is the Markov Chain. A shows the first 50 iterations. The chains have not converged. B shows the first 1000 iterations. All chains have converged. C shows the last 500 iteration of the Markov Chain. They represent a set of draws from the target distribution. No points are overlaying each others. From [13]

there they are doing steps according to the Metropolis algorithm exploring the parameter space. The positions each chain took are indicated by the black lines. As there two parameters, the chains in this case move in a two-dimensional parameter space. Increasing the amounts of parameters increases the dimensions of the parameter space accordingly. In this example, the two parameter both follow normal posterior distribution with mean zero, $N \sim \mathcal{N}(0, I)$. Following the Metropolis algorithms, all the chains converge to the parameter space that is described by the normal posterior distribution, see B in Fig.33. Removing the chains and adding a point for every position visited yields Fig.33 C. These points then build the posterior given by the Bayesian inference. The algorithms used in Stan are working on a similar principle. Chains are used to explorer the parameter space to be able to describe the posterior distribution of the parameters.

The HMC uses an approximate Hamiltonian dynamics simulation to suppress local random walk behaviour used by other algorithm such as the Metropolis algorithm. That allows for the HMC to move more rapidly through the target distribution.

In HMC every θ_j is assigned an auxiliary momentum variable ρ. Both θ and ρ are then updated together. The posterior distribution $p(\theta|y)$ is augmented by the independent distribution $p(\rho)$, defining the joint distribution as

$$p(\rho, \theta|y) = p(\rho)p(\theta|y). \tag{C.1}$$

From this simulation only θ is of interest for us. The inclusion of ρ is merely there to help the algorithm move fast through the parameter space.

In Stan the auxiliary momentum distribution is a multivariate normal that does not depend on the parameters θ. It has a mean of 0 and the variance is given by the Euclidean metric or mass matrix M,

$$\rho \sim \mathcal{N}(0, \mathrm{M}). \tag{C.2}$$

Stan sets M^{-1} equal to a diagonal estimate of the covariance computed during the warm up.
From the joint distribution $p(\rho, \theta)$ a Hamiltonian can be derived,

$$H(\rho, \theta) = -\log p(\rho|\theta) - \log p(\theta) = T(\rho|\theta) + V(\theta). \tag{C.3}$$

Evolving the system via Hamilton's equations for θ and ρ leaves a two state differential equations that needs to be solved,

$$\frac{d\theta}{dt} = +\frac{\partial T}{\partial \rho} \tag{C.4a}$$

$$\frac{d\rho}{dt} = -\frac{\partial V}{\partial \theta}. \tag{C.4b}$$

To solve these equations Stan uses the leapfrog integrator which is a numerical integration algorithm that is specifically adapted to provide stable results for Hamiltonian systems of equations. Each iteration of the HMC consists of three steps:

1. A random ρ is drawn from its posterior distribution, Eq.C.2

2. The θ and ρ are updated simultaneously solving Eqs.C.4 using the leapfrog integrator. The leap frog step is repeated L times, each scaled by a factor ϵ:

$$\rho \leftarrow \rho - \frac{\epsilon}{2}\frac{\partial V}{\partial \theta} \tag{C.5a}$$

$$\theta \leftarrow \theta + \epsilon M^{-1}\rho \tag{C.5b}$$

$$\rho \leftarrow \rho - \frac{\epsilon}{2}\frac{\partial V}{\partial \theta} \tag{C.5c}$$

3. After all L steps are done parameter a Metropolis acceptance step is done. The probability of keeping the generated (ρ^*,θ^*) generated from (ρ,θ) is given by

$$\min(1, \exp(H(\rho, \theta) - H(\rho^*, \theta^*))). \tag{C.6}$$

   If the step is not accepted the previous parameters are returned for the next draw and used for the next iteration.

For the HMC the discretization time ϵ, the metric M and number of leap frog steps L need to be specified. The sampling efficiency of the of the algorithm is highly sensitive

to the choice of these three parameters. To avoid this problem, the No-U turn sampler (NUTS) has been developed [26]. The workings of NUTS are described in [26].
To use the NUTS for the sampling of the Bayesian inference no arguments need to be given besides the ones for the Bayesian inference. Optional the `max_treedpeth` of the NUTS can be adjusted. By default it is set to ten.